Progress in Time-Dependent Density-Functional Theory

M.E. Casida and M. Huix-Rotllant

Laboratoire de Chimie Théorique, Département de Chimie Moléculaire, Institut de Chimie Moléculaire de Grenoble, Université Joseph Fourier, BP 53, F-38041 Grenoble Cedex 9, France; email: mark.casida@ujf-grenoble.fr, miquel.huix@ujf-grenoble.fr

Annu. Rev. Phys. Chem. 2012. 63:287–323

First published online as a Review in Advance on January 13, 2012

The *Annual Review of Physical Chemistry* is online at physchem.annualreviews.org

This article's doi: 10.1146/annurev-physchem-032511-143803

0066-426X/12/0505-0287$20.00

Keywords

adiabatic approximation, memory, electronic excited states, photochemistry, excitons

Abstract

The classic density-functional theory (DFT) formalism introduced by Hohenberg, Kohn, and Sham in the mid-1960s is based on the idea that the complicated *N*-electron wave function can be replaced with the mathematically simpler 1-electron charge density in electronic structure calculations of the ground stationary state. As such, ordinary DFT cannot treat time-dependent (TD) problems nor describe excited electronic states. In 1984, Runge and Gross proved a theorem making TD-DFT formally exact. Information about electronic excited states may be obtained from this theory through the linear response (LR) theory formalism. Beginning in the mid-1990s, LR-TD-DFT became increasingly popular for calculating absorption and other spectra of medium- and large-sized molecules. Its ease of use and relatively good accuracy has now brought LR-TD-DFT to the forefront for this type of application. As the number and the diversity of applications of TD-DFT have grown, so too has our understanding of the strengths and weaknesses of the approximate functionals commonly used for TD-DFT. The objective of this article is to continue where a previous review of TD-DFT in Volume 55 of the *Annual Review of Physical Chemistry* left off and highlight some of the problems and solutions from the point of view of applied physical chemistry. Because doubly-excited states have a particularly important role to play in bond dissociation and formation in both thermal and photochemistry, particular emphasis is placed on the problem of going beyond or around the TD-DFT adiabatic approximation, which limits TD-DFT calculations to nominally singly-excited states.

1. INTRODUCTION

Ab initio: Latin meaning from the beginning; used in quantum chemistry for first principles wave-function calculations but often includes DFT in other contexts

TD: time dependent

DFT: density-functional theory

LR: linear response

Even after the Born-Oppenheimer separation, the time-independent Schrödinger equation for N electrons in an "external potential" consisting of M nuclei and any applied electric fields, $\hat{H}\,\Psi(1,2,\ldots,N) = E\Psi(1,2,\ldots,N)$, is still notoriously difficult to solve. Yet such amazing progress has been made in solving this equation for increasingly complex systems since its introduction early in the twentieth century that we may well refer to that period as the century of quantum mechanics. Some, but by no means all, of this progress may be explained by improvements in computing machines. Improved approximation methods based on progress in our understanding of the mathematical and physical properties of the underlying objects of quantum mechanics have also helped us to treat increasingly complex systems by providing more efficient solution methods. One of the landmarks has been the Hohenberg-Kohn-Sham (1, 2) density-functional theory (DFT),[1] in which the complicated many-electron wave function, $\Psi(1,2,\ldots,N)$, may be replaced with functionals of a simpler object—namely the charge density, $\rho(\mathbf{r}_1) = N\sum_{\sigma_1}\int\int\cdots\int|\Psi(\mathbf{r}_1\sigma_1,2,\ldots,N)|^2 d2d3\cdots dN$—to calculate properties of the ground-stationary state.[2] DFT was a mighty advance, but until the 1980s, it remained largely in the shadow of wave-function theory as far as quantum chemistry was concerned. By then, approximate exchange-correlation functionals had advanced to the point where they could often compete with accurate ab initio wave-function methods, particularly for larger molecules of experimental interest. Nevertheless, the restriction to the ground-stationary state was clearly disappointing for such popular applications as UV-visible spectroscopy, nonlinear optics, and photochemistry. But, as with most things, "it was all just a matter of time" before things shifted. The formal basis of modern time-dependent (TD) DFT is the Runge-Gross theorem showing that, for a system initially in its ground stationary state exposed to a TD perturbation, the TD charge density, $\rho(\mathbf{r},t)$, determines the TD external potential up to an additive function of time (3). Once again, a formally exact functional must be approximated, but this one gives immediate access to nonlinear optics properties and, via linear-response (LR) theory, to excited-state information. The LR-TD-DFT equations introduced by one of us (4) have been programmed in most quantum chemistry and quantum physics electronic structure codes and are currently the mostly widely used method to treat the excited states of medium- to large-sized molecules. Many review articles have been written on various aspects of TD-DFT, some special volumes devoted to TD-DFT have appeared or will soon appear, and three books have been published or will soon be published (see the additional references cited in Reference 5, as well as more recent citations in References 6 and 7). The present review may be regarded as a follow-up to an earlier review of TD-DFT in this journal (8).

We take the point of view of theoretical physical chemists interested in spectroscopy and photoprocesses and particular emphasis is given to advances made over the past seven years. **Figure 1** provides a schematic summary, sampling the breadth of chemical and physical phenomena that physical chemists may describe and including features to which we often refer. We also often take pains to first review wave-function theory before discussing (TD-)DFT. Our aim in so doing is to provide a subsequent discussion concentrating more fully on the difference between (TD-)DFT and wave-function theory.

This review is organized as follows: The next section reviews elementary wave-function theory. Because TD-DFT shares many features in common with DFT and problems in approximate

[1] A functional is a function of a function. It is designated by a square-bracket notation. Thus $v[\rho](\mathbf{r})$ is simultaneously a functional of the function ρ and a function of the position, $\mathbf{r}$. Unless explicitly present, we take $\hbar = m_e = e = 1$ (i.e., we use Hartree atomic units) throughout this article.

[2] Within this text, space and spin coordinates have been denoted by $1, 2, \cdots = \mathbf{r}_1\sigma_1, \mathbf{r}_2\sigma_2, \ldots$.

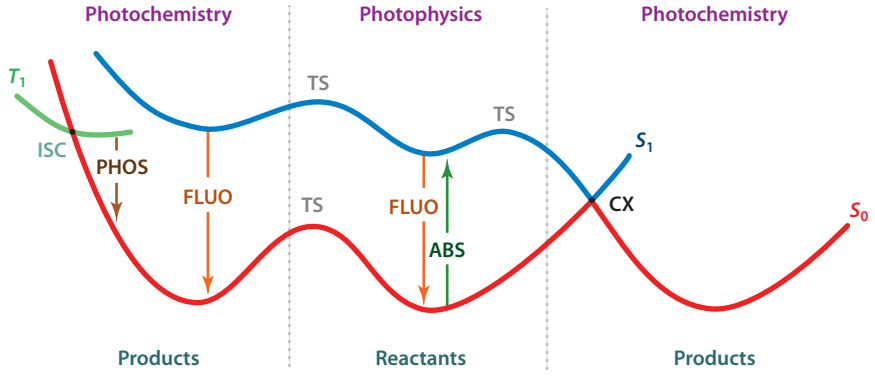

Figure 1

Schematic representation of potential energy surfaces for photophysical and photochemical processes: ABS, absorption; CX, conical intersection; FLUO, fluorescence; ISC, intersystem crossing; PHOS, phosphorescence; S_0, ground singlet state; S_1, lowest excited singlet state; T_1, lowest triplet state; TS, transition state.

functionals used in TD-DFT may often be traced back to problems inherited from approximate functionals in DFT, Section 3 reviews conventional time-independent ground-state DFT. Section 4 then introduces formal TD-DFT; the adiabatic approximation (AA), which defines conventional TD-DFT; and typical applications. It then discusses problems with conventional TD-DFT, how to test for problems, and how problems can be fixed or at least attenuated. Some of these problems come from the very nature of the TD-DFT AA. TD-DFT should be exact so long as the exact frequency- and initial state-dependent exchange-correlation (xc) functional of TD-DFT is used. This is not the same as the xc-functional of ordinary DFT, which is borrowed by TD-DFT whenever the AA is used; thus, a true TD-DFT xc-functional should go beyond the AA to include frequency and possibly also initial state dependence. Section 5 discusses what is known about the exact xc-functional of TD-DFT and discusses attempts at creating and using approximate functionals that go beyond the TD-DFT AA. As these attempts are in an embryonic stage, it is also interesting to consider practical working methods to overcome the limitations of the TD-DFT AA without introducing any frequency dependence. This is the topic addressed in Section 6. Section 7 sums up with some perspectives regarding future developments in TD-DFT.

2. WAVE-FUNCTION THEORY

Modern DFT and TD-DFT resemble wave-function theory in its simplest incarnations. For this reason, it is useful to review basic wave-function theory, if only to establish some notation and to make sure that key concepts are fresh in the mind of the reader.

2.1. Hartree-Fock Approximation

According to basic quantum mechanics, the wave function, Ψ, describes the fundamental state of the system, so we should aim to solve the Schrödinger equation. Except for exceptionally simple systems, we can solve the Schrödinger equation only approximately with the help of powerful approximation techniques such as the well-known variational principle.

The Hartree-Fock (HF) approximation consists of using a trial wave function in the form of a single Slater determinant of orthonormal orbitals. Variational minimization of the energy subject

AA: adiabatic approximation

xc: exchange-correlation

HF: Hartree-Fock

to the orbital orthonormality constraint leads to the HF equation,

$$\hat{f}\psi_i(1) = \varepsilon_i \psi_i(1), \tag{1}$$

SCF: self-consistent field

1-RDM: one-electron reduced-density matrix

EOM: equation-of-motion

given in a spin-orbital notation. Here, the one-electron Fock operator, $\hat{f}$, is the sum of the one-electron kinetic energy operator, $\hat{t}$, and the external potential, $v_{ext}(\mathbf{r})$, which is a multiplicative operator describing the interaction of the electron with the electric fields generated by the M nuclei and any applied electronic fields. The Fock operator also includes a self-consistent field (SCF) composed of a Hartree term (also known as the Coulomb term), $v_H(\mathbf{r}_1) = \int \rho(\mathbf{r}_2)/\mathbf{r}_{12}\, d\mathbf{r}_2$, and an exchange operator, $\hat{\Sigma}_x$ (designated here as the exchange self-energy using the terminology and notation of Green's function theory). As described in elementary quantum chemistry textbooks,

$$\hat{\Sigma}_x\phi(1) = -\int \frac{\gamma(1,2)}{r_{12}}\phi(2)\, d2 \tag{2}$$

is a complicated integral operator, where $\gamma(1,2) = \sum_i \psi_i(1) n_i \psi_i^*(2)$ is the one-electron reduced-density matrix (1-RDM) and the n_i are orbital occupation numbers. For completeness, we note the HF energy expression for the total energy:

$$E = \sum_i n_i \langle \phi_i | \hat{t} | \phi_i \rangle + \int v_{ext}(\mathbf{r})\rho(\mathbf{r})\, d\mathbf{r} + E_H[\rho] + E_x[\gamma], \tag{3}$$

where $\hat{t}$ is the one-electron kinetic energy operator, v_{ext} is any potential (i.e., the nuclear attraction and any applied electric fields) external to the system of N-electrons, the Hartree energy,

$$E_H[\rho] = \frac{1}{2}\int\int \frac{\rho(\mathbf{r}_1)\rho(\mathbf{r}_2)}{r_{12}} d\mathbf{r}_1\, d\mathbf{r}_2, \tag{4}$$

and the exchange energy,

$$E_x[\gamma] = -\frac{1}{2}\int\int \frac{|\gamma(1,2)|^2}{r_{12}} d1 d2. \tag{5}$$

According to Koopmans's theorem (9), the occupied orbital energies, ε_i, in Equation 1 may be interpreted as minus ionization potentials and the unoccupied orbital energies as minus electron affinities. That is, occupied orbitals "see" $N-1$ electrons, whereas unoccupied orbitals "see" N electrons.

2.2. Excited States

Let us now turn to the excited-state problem. We begin with the equation-of-motion (EOM) formalism. This has the advantage of conceptual simplicity and, though we do not show it here, can be directly linked to LR theory (10). The operator, $|I\rangle\langle 0|$, which destroys the ground state ($|0\rangle$) and creates the Ith excited state ($|I\rangle$) and its adjoint, $|0\rangle\langle I|$, are solutions of the EOM:

$$[\hat{H}, \mathcal{O}^\dagger] = \omega\hat{\mathcal{O}}^\dagger. \tag{6}$$

Thus, $\omega = E_I - E_0$ is an excitation energy in the case of $|I\rangle\langle 0|$ and $\omega = E_0 - E_I$ is a de-excitation in the case of $|0\rangle\langle I|$.

We now seek a solution of the EOM of the form

$$\hat{\mathcal{O}}^\dagger = \sum_{i,a} a^\dagger i X_{ia} + \sum_{i,a} i^\dagger a Y_{ia}. \tag{7}$$

Accordingly, we develop $\hat{\mathcal{O}}^\dagger$ in a basis set of one-particle/one-hole (1p1h) excitation and de-excitation operators. This operator basis and the EOM operator "metric" defined by

$(\hat{\mathcal{A}}|\hat{\mathcal{B}}) = \langle\Phi_{HF}|[\hat{\mathcal{A}}^\dagger, \hat{\mathcal{B}}]|\Phi_{HF}\rangle$ then allow us to develop a matrix form of the EOM, namely,

$$\begin{bmatrix} \mathbf{A} & \mathbf{B} \\ \mathbf{B}^* & \mathbf{A}^* \end{bmatrix} \begin{pmatrix} \vec{X} \\ \vec{Y} \end{pmatrix} = \omega \begin{bmatrix} \mathbf{1} & \mathbf{0} \\ \mathbf{0} & -\mathbf{1} \end{bmatrix} \begin{pmatrix} \vec{X} \\ \vec{Y} \end{pmatrix}, \tag{8}$$

where the notation $\vec{X}$ and $\vec{Y}$ are deliberately chosen to indicate that these objects are to be treated as column vectors in Equation 8. The matrices are defined by

$$\begin{aligned} A_{ia,jb} &= \delta_{i,j}\delta_{a,b}(\varepsilon_a - \varepsilon_i) + K_{ia,jb} \\ B_{ia,jb} &= K_{ia,bj}, \end{aligned} \tag{9}$$

where the coupling matrix is

$$K_{pq,rs} = (pq|f_H|sr) - (pr|f_H|sq). \tag{10}$$

Note that here and henceforth we adapt the molecular orbital (MO) index convention

$$\underbrace{a, b, c, \ldots, g, h}_{unoccupied}\ \underbrace{i, j, k, l, m, n}_{occupied}\ \underbrace{o, p, q, \ldots, y, z}_{free}, \tag{11}$$

where "free" means "free to be either occupied or unoccupied." We also use both a "lazy version" of second-quantized notation where $p = \hat{a}_p$ and $p^\dagger = \hat{a}_p^\dagger$ and Mulliken "charge cloud" notation

$$(pq|f|sr) = \int\int \psi_p^*(1)\psi_q(1) f(1,2)\psi_s^*(2)\psi_r(2) d1 d2, \tag{12}$$

where we take f to be the Hartree kernel, $f_H(1,2) = 1/r_{12}$.

Equation 8 is often called the random-phase approximation (RPA)[3] for purely historical reasons. Some caution is in order when using this term, given that the RPA was originally developed in nuclear and solid-state physics without the second integral in the coupling matrix (Equation 10). Although we have chosen an EOM derivation of Equation 10, this equation also emerges from LR-TD-HF and so may be referred to by that name (see, for example, Reference 10, pp. 122–34, 144–51). It is a pseudoeigenvalue problem with an operator "overlap matrix" on the right-hand side that is simplectic rather than positive definite as would be a true overlap matrix. It also has paired excitation, $(\vec{X}, \vec{Y})$, and de-excitation solutions, $(\vec{Y}^*, \vec{X}^*)$, whose corresponding excitation/de-excitation energies, ω, differ by only a sign change. The normalization of the solutions is given by $(\hat{\mathcal{O}}^\dagger|\hat{\mathcal{O}}^\dagger) = \vec{X}^\dagger\vec{X} - \vec{Y}^\dagger\vec{Y}$, which is typically positive for excitations and negative for de-excitations. Potential energy surfaces (PESs) may be calculated from the excited-state energies, $E_I = E_{HF} + \omega_I$. Because analytic derivatives are available for LR-TD-HF (11), automatic searching for critical points on excited-state PESs (**Figure 1**) is possible in this model.

Important to note is that the LR-TD-HF equation provides not only excitation energies, ω_I, but also the corresponding oscillator strengths,

$$f_I = \frac{2m_e}{3\hbar}\omega_I|\langle 0|\mathbf{r}|I\rangle|^2, \tag{13}$$

which may be calculated from the coefficient vector, $(\vec{X}, \vec{Y})$, and the dipole matrix. Oscillator strengths are pure numbers, and in a complete basis set (or other basis set satisfying the relation $[x, \hat{p}_x] = +i\hbar$), they satisfy the Thomas-Reiche-Kuhn f-sum rule, $\sum_I f_I = N$, where N is the number of electrons. Equation 13 has been deliberately expressed in Gaussian, rather than atomic, units so that it may be more easily related to the molar extinction coefficient, ε, in an

MO: molecular orbital

RPA: random-phase approximation

PES: potential energy surface

[3] Sometimes one talks of RPA with exchange (RPAE or RPAX) to emphasize inclusion of the second integral in Equation 10. However, it is often left to the reader to figure out whether this integral is included in the term RPA.

absorption experiment. In Système International units, the frequency spectrum is given to a first approximation by

$$\varepsilon(\nu) = \sum_I \frac{N_A e^2}{4 m_e c \ln(10) \varepsilon_0} \mathcal{S}(\nu - \nu_I)$$
$$= (6.94 \times 10^{+18}\,\mathrm{L/cm.s}) \sum_I \mathcal{S}(\nu - \nu_I), \quad (14)$$

where N_A is Avogadro's number and $\mathcal{S}(\nu)$ is a spectral shape function (typically a Gaussian whose area is normalized to unity and whose full-width-at-half-maximum is determined from experiment).

TDA: Tamm-Dancoff approximation

TOTEM: two-orbital two-electron model

The Tamm-Dancoff approximation (TDA) is frequently made and consists of neglecting the **B** matrix in the LR-TD-HF equation, thus decoupling the excitations from the de-excitations. The Thomas-Reiche-Kuhn *f*-sum rule is lost when the TDA is made, but the resultant equation is variational in terms of the wave function. In particular, the minimal acceptable model for the excited states of a closed-shell molecule is configuration interaction singles (CIS) in which the excited-state wave function is taken to be a linear combination of 1p1h (singly excited) HF configurations, $\Phi_I^{CIS} = \sum_{i,a} a^\dagger i \Phi_{HF} C_{ia,I} = \hat{O}_I^\dagger \Phi_{HF}$. Use of the variational principle to find the coefficients that minimize the energy then yields

$$\mathbf{A}\vec{X}_I = \omega_I \vec{X}_I, \quad (15)$$

where $\vec{C}_I$ has been renamed $\vec{X}_I$ and the notations $\mathbf{A} = \mathbf{H} - E_{HF}$ and $\omega_I = E_I - E_{HF}$ have been introduced to make the correspondence with the TDA of LR-TD-HF clear. Because of the variational nature of the TDA, for some applications, this "approximation" sometimes gives better results than the original RPA equation (see below).

It is useful for interpretational purposes to restrict ourselves to the case where an electron is excited from an initial MO *i* to a target MO *a* neglecting any orbital relaxation. This two-orbital two-electron model (TOTEM) corresponds to the spin-preserving excitations in **Figure 2** and yields one singlet and one triplet excitation energy, as shown in **Table 1**.

The CIS expressions of **Table 1** may also be derived in a more direct way using the multiplet sum method (MSM) as follows: The wave functions in **Figure 2** are all eigenfunctions of the spin operator $\hat{S}_z$ but not necessarily of $\hat{S}^2$. Linear combinations, Φ_{S,M_S}, are needed to form simultaneous

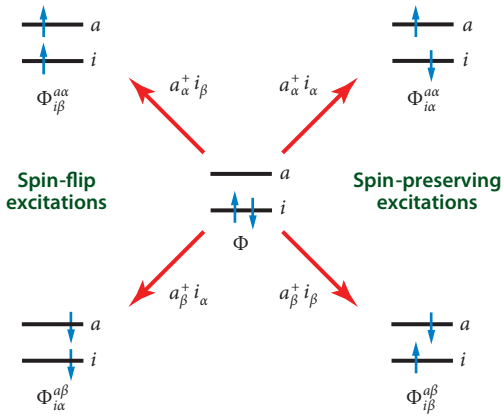

Figure 2

Schematic of excitations in the two-orbital two-electron model, showing both spin-flip excitations (*left*) and spin-preserving excitations (*right*).

Table 1 Summary of formulae within the two-orbital two-electron model (Figure 2)

ΔSCF	CIS (TDA-TD-HF)
$I_i = \varepsilon_i$	$I_i = \varepsilon_i$
$A_a = \varepsilon_a$	$A_a = \varepsilon_a$
$A_a(i^{-1}) = A_a - (aa\|f_H\|ii) + (ai\|f_H\|ia)$	$A_a(i^{-1}) = A_a - (aa\|f_H\|ii) + (ai\|f_H\|ia)$
$\omega_M = \varepsilon_a - \varepsilon_i - (aa\|f_H\|ii) + (ai\|f_H\|ia)$	$\omega_M = \varepsilon_a - \varepsilon_i - (aa\|f_H\|ii) + (ai\|f_H\|ia)$
$\omega_T = \omega_M - (ia\|f_H\|ai)$	$\omega_T = \omega_M - (ia\|f_H\|ai)$
$\omega_S = \omega_M + (ia\|f_H\|ai)$	$\omega_S = \omega_M + (ia\|f_H\|ai)$
Linearized ΔSCF DFT	**TDA-TD-DFT**
$I_i = \varepsilon_i - \frac{1}{2}(ii\|f_H + f_{xc}^{\uparrow,\uparrow}\|ii)$	$I_i = \varepsilon_i$
$A_a = \varepsilon_a + \frac{1}{2}(aa\|f_H + f_{xc}^{\uparrow,\uparrow}\|aa)$	$A_a = \varepsilon_a + (aa\|f_H\|ii) + (ai\|f_{xc}^{\uparrow,\uparrow}\|ia)$
$A_a(i^{-1}) = A_a - (aa\|f_H + f_{xc}^{\uparrow,\uparrow}\|ii)$	$A_a(i^{-1}) = A_a - (aa\|f_H\|ii) + (ai\|f_H\|ia)$
$\omega_M = \varepsilon_a - \varepsilon_i + \frac{1}{2}(aa - ii\|f_H + f_{xc}^{\uparrow,\uparrow}\|aa - ii)$	$\omega_M = \varepsilon_a - \varepsilon_i + (ai\|f_H + f_{xc}^{\uparrow,\uparrow}\|ia)$
$\omega_T = \omega_M + (aa\|f_{xc}^{\uparrow,\uparrow} - f_{xc}^{\uparrow,\downarrow}\|ii)$	$\omega_T = \omega_M - (ia\|f_H + f_{xc}^{\uparrow,\downarrow}\|ai)$
$\omega_S = \omega_M - (aa\|f_{xc}^{\uparrow,\uparrow} - f_{xc}^{\uparrow,\downarrow}\|ii)$	$\omega_S = \omega_M + (ia\|f_H + f_{xc}^{\uparrow,\downarrow}\|ai)$

I_i is minus the ionization potential of orbital i. A_a is minus the electron affinity of orbital a. A_a (i^{-1}) is minus the electron affinity of orbital a for the ion formed by removing an electron from orbital i. ω_T, ω_S, and ω_M are, respectively, $i \to a$ excitation energies to the triplet, singlet, and mixed symmetry states. The mixed symmetry state has energy $\omega_M = A_a\,(i^{-1}) - I_i$. ΔSCF quantities are obtained by the usual multiplet sum procedure (12) except that a truncated Taylor expansion of the xc-functional has been used in the DFT case (13). The identification of I_i and A_a in the TD-DFT case is based on OEP theory (14).

eigenvectors of the two operators:

$$\begin{aligned} \Psi_{0,0} &= \frac{1}{\sqrt{2}}(\Phi_{i\alpha}^{a\alpha} + \Phi_{i\beta}^{a\beta}), \quad \Psi_{1,-1} = \Phi_{i\alpha}^{a\beta} \\ \Psi_{1,0} &= \frac{1}{\sqrt{2}}(\Phi_{i\alpha}^{a\alpha} - \Phi_{i\beta}^{a\beta}), \quad \Psi_{1,+1} = \Phi_{i\beta}^{a\alpha}, \end{aligned} \tag{16}$$

where $\Phi_{1,-1}$, $\Phi_{1,0}$, and $\Phi_{1,+1}$ are degenerate triplet states and $\Phi_{0,0}$ is an open-shell singlet state. The triplet energy is easily expressed as the expectation value of a single determinant,

$$E_T = \langle\Psi_{1,-1}|\hat{H}\,|\Psi_{1,-1}\rangle = \langle\Phi_{i\alpha}^{a\beta}|\hat{H}\,|\Phi_{i\alpha}^{a\beta}\rangle = E[\Phi_{i\alpha}^{a\beta}]. \tag{17}$$

The MSM allows the singlet energy, E_S, also to be expressed in terms of expectation values of single determinant wave functions. To do so, we note that

$$\begin{aligned} E_S &= \langle\Psi_{0,0}|\hat{H}\,|\Psi_{0,0}\rangle = \langle\Phi_{i\alpha}^{a\alpha}|\hat{H}\,|\Phi_{i\alpha}^{a\alpha}\rangle + \langle\Phi_{i\alpha}^{a\alpha}|\hat{H}\,|\Phi_{i\beta}^{a\beta}\rangle \\ E_T &= \langle\Psi_{1,0}|\hat{H}\,|\Psi_{1,0}\rangle = \langle\Phi_{i\alpha}^{a\alpha}|\hat{H}\,|\Phi_{i\alpha}^{a\alpha}\rangle - \langle\Phi_{i\alpha}^{a\alpha}|\hat{H}\,|\Phi_{i\beta}^{a\beta}\rangle. \end{aligned} \tag{18}$$

Eliminating the cross term and using Equation 17 gives us

$$\begin{aligned} E_S &= 2\langle\Phi_{i\alpha}^{a\alpha}|\hat{H}\,|\Phi_{i\alpha}^{a\alpha}\rangle - \langle\Phi_{i\alpha}^{a\beta}|\hat{H}\,|\Phi_{i\alpha}^{a\beta}\rangle \\ &= 2E[\Phi_{i\alpha}^{a\alpha}] - E[\Phi_{i\alpha}^{a\beta}], \end{aligned} \tag{19}$$

where the last line emphasizes that the singlet energy has now been expressed uniquely in terms of the energies of single Slater determinants. Subtracting the ground-state HF energy, E_{HF}, and explicitly evaluating the various single-determinantal energies leads to the CIS formulae in **Table 1**.

MSM: multiplet sum method

Unfortunately, the CIS formulae in **Table 1** are poor approximations for the singlet and triplet excitation energies because, per Koopmans' theorem, HF orbital energies are preprepared

STEX: static exchange

SODS: same-orbitals-for-different-spins

DODS: different-orbitals-for-different-spins

to describe ionization and electron attachment rather than neutral excitations. It would be better to begin with a zero-order picture where both the initial and target orbitals "see" $N-1$ electrons. This is the idea behind the static exchange (STEX) method (15) where the excitations of a neutral molecule that begin with MO i are carried out by first performing a calculation on the cation with one electron removed from the MO i (denoted by the abbreviated configuration, i^{-1}). The associated unoccupied cation MO creation operators, $a^\dagger(i^{-1})$, are then used together with the occupied neutral MO destruction operators, i, to carry out a variational calculation with a wave function of the form $\Psi = \sum_a a^\dagger(i^{-1})i\,\Phi_{HF}$. Applying this idea to the TOTEM gives the following STEX formulae:

$$\begin{aligned} \omega_M &= A_a(i^{-1}) - I_i \\ \omega_S &= \omega_M + (ia|f_H|ai) \\ \omega_T &= \omega_M - (ia|f_H|ai), \end{aligned} \tag{20}$$

where the singlet, ω_S, and triplet, ω_T, excitation energies have been expressed in terms of an excitation to a fictitious single-determinantal state of mixed symmetry whose excitation energy, ω_M, is equal to the difference between minus the electron affinity of the i^{-1} cation, $A_a(i^{-1})$, and minus the ionization potential of the MO i, I_i. Specific CIS values are given in **Table 1**.

So, what happens for a charge-transfer excitation between two neutral molecules located at a distance R apart, where R is assumed to be large? According to Equation 20, we have $\omega_T \approx \omega_M \approx \omega_S$ when the differential overlap $\psi_i(\mathbf{r})\psi_a(\mathbf{r})$ becomes negligible. From Koopmans' theorem and the CIS results in **Table 1**, we see that $\omega_M \approx A_a - I_i - 1/R$ as would be expected on physical grounds. That is, the excitation energy required to transfer an electron from MO i to MO a over a distance R is the energy needed to ionize the electron from MO i plus the energy recuperated from adding it into MO a and from the electrostatic attraction of the two ions.

2.3. Stability Analysis and Bond Breaking

Most HF calculations are restricted HF calculations with the same-orbitals-for-different-spins (SODS), as opposed to different-orbitals-for-different-spins (DODS). In addition, they assume real MOs, each of which belongs to an irreducible representation of the molecular point group. Unrestricted HF consists of dropping the restriction of the same orbitals for different spin, but it typically uses real MOs. As unrestricted HF calculations are more general than restricted HF calculations, cases arise where unrestricted HF calculations give an energy lower than that provided by restricted HF calculations by allowing spatial symmetry breaking. Because the iterations in the HF SCF calculation typically preserve symmetry for closed-shell molecules, finding unrestricted HF calculations with lower energy than that of restricted HF calculations typically requires explicit symmetry breaking to be introduced during the iterations. By contrast, such symmetry breaking can, for example, be a simple way to dissociate H_2 into neutral atoms, $H\uparrow + H\downarrow$, which is often a good approximation to the correct dissociation into a structure, $[H\uparrow + H\downarrow \leftrightarrow H\downarrow + H\uparrow]$, with equal probability for finding each spin on each atom. Generalized HF removes all restrictions on the HF orbitals, demonstrating an intimate relationship between restricted HF stability analysis and LR-TD-HF.

Symmetry breaking will occur when an orbital unitary transformation $\psi_r^\lambda(\mathbf{r}) = e^{\lambda\hat{U}^*}\psi_r(\mathbf{r}) = e^{i\lambda(\hat{R}+i\hat{I})}\psi_r(\mathbf{r})$ leads to energy lowering:

$$\begin{aligned} E_\lambda &= E_0 + \tfrac{\lambda^2}{2}\begin{pmatrix}\vec{U}^{\dagger *} & \vec{U}^{\dagger}\end{pmatrix}\begin{bmatrix}\mathbf{A} & \mathbf{B}\\ \mathbf{B} & \mathbf{A}\end{bmatrix}\begin{pmatrix}\vec{U}\\ \vec{U}^{*}\end{pmatrix} + \mathcal{O}^{(3)}(\lambda) \\ &= E_0 + \lambda^2[\vec{R}^\dagger(\mathbf{A}-\mathbf{B})\vec{R} + \vec{I}^\dagger(\mathbf{A}+\mathbf{B})\vec{I}] + \mathcal{O}^{(3)}(\lambda), \end{aligned} \tag{21}$$

where the **A** and **B** matrices are the same as previously defined in Equation 9 except that they are real because we are beginning with a restricted HF solution with real orbitals. Equation 8 can always be put into the form $(\mathbf{A}+\mathbf{B})(\mathbf{A}-\mathbf{B})\vec{Z}=\omega\vec{Z}$, where $\vec{Z}=\vec{X}-\vec{Y}$, making immediately evident the understanding that an imaginary LR-TD-HF excitation energy means that one or both of the matrices $\mathbf{A}+\mathbf{B}$ and $\mathbf{A}-\mathbf{B}$ have negative eigenvalues and thus that the restricted HF solution is variationally unstable because there is some choice of the vectors $\vec{R}$ and $\vec{I}$, which will further lower the restricted HF energy. The most common of these is the so-called triplet instability, where the imaginary energy is associated with a triplet excitation energy. However, other types of instabilities are possible. For a more complete analysis, see Reference 16.

DFA: density-functional approximation

Note that imaginary excitation energies can never occur when the LR-TD-HF equation is solved in the TDA. In fact, the variational nature of CIS does much to prevent the unphysical plunges of excitation energies that are often seen in LR-TD-HF as, say, singlet near instabilities associated with triplet instabilities. Thus, the TDA is a partial solution to the LR-TD-HF instability problem.

Physically, LR-TD-HF is giving nonsensical excitation energies because it is based on the response of an unphysical ground-state wave function. In fact, although the HF approximation is often a good starting point for closed-shell molecules at their ground-state equilibrium geometry—i.e., it may be reasonable around the minima on the ground-state curve in **Figure 1**—the same approximation is notorious for failing at transition states where bonds are being made or broken. In such cases, the minimum acceptable description is a wave function that is a linear combination of the reactant, Φ_R, and product, Φ_P, trial wave functions, $\Phi=\Phi_R C_R+\Phi_P C_P$. Typically, this involves some sort of configuration mixing between the ground-state determinant and a two-particle/two-hole (2p2h) (doubly) excited state. Though there is no transition state on the ground-state curve, the dissociation of the H(1*s*)-H(1*s*) σ-bond is a textbook case. The minimum acceptable correctly dissociating description of the ground-state wave function, satisfying all the spatial and spin symmetry rules, is a trial function of the form $\Psi=|\sigma_g\bar{\sigma}_g|C_1+|\sigma_u\bar{\sigma}_u|C_2$, where σ_g is the familiar bonding MO and σ_u is the familiar antibonding MO. The coefficients $C_1=1/\sqrt{2}=-C_2$ give the proper neutral, $H_2\rightarrow[H\uparrow+H\downarrow\leftrightarrow H\downarrow+H\uparrow]$, dissociation limit of the ground $X^1\Sigma_g$ state. The combination $C_1=1/\sqrt{2}=C_2$ gives the proper ionic dissociation limit, $H_2\rightarrow[H:^-+H^+\leftrightarrow H^++H:^-]$, of the 2p2h $1^1\Sigma_g$ state. Though the $1^1\Sigma_g$ state is dominated in this simple model by the 2p2h configuration at the ground-state equilibrium geometry, the fact that neither C_1 nor C_2 are zero in the dissociation limit indicates that configuration mixing of the ground and 2p2h excited-state configurations is occurring. In fact, the simplest wave-function model for breaking of any homoleptic single bond involves mixing of the ground-state configuration with a 2p2h configuration.

3. CLASSIC DENSITY-FUNCTIONAL THEORY

It is difficult (possibly impossible) to speak of TD-DFT without first saying a word about ordinary DFT, otherwise known as the classic DFT of the ground stationary state, which is also the static limit of TD-DFT. Because our focus here is not on DFT, which is fairly well known, we keep this section short. Readers interested in more information about DFT may choose to consult any one of a number of books on the subject, such as, for example, that of Dreizler & Gross (17).

Before going further, it is important to make the distinction between DFT and density-functional approximations (DFAs). DFT is a formalism that provides existence theorems showing that there is something well defined to be approximated. However, from a practical point of view, DFT is useless unless DFAs can be found that are simpler to use than the wave-function theory of corresponding accuracy. The search for pragmatic approximations, ideally guided by

rigorous formal DFT but occasionally borrowing from wave-function theory, pervades all of density-functional culture.

3.1. Formalism

Hohenberg and Kohn set down the basic formalism of modern DFT in two theorems (1). The first Hohenberg-Kohn theorem states that the ground-state charge density of a system of interacting electrons determines the external potential up to an arbitrary additive constant. Because integrating over the charge density gives the number of electrons, this implies that the ground-state charge density determines the Hamiltonian up to an additive constant (i.e., the arbitrary zero of the energy) and hence determines almost everything about the ground and excited states of the system.

In fact, the ground-state density must also determine the dynamic LR of the ground stationary state,

$$\chi(\mathbf{r}_1, \mathbf{r}_2; \omega) = \int_{-\infty}^{+\infty} e^{+i\omega(t_1 - t_2)} \frac{\delta\rho(\mathbf{r}_1, t_1)}{\delta v_{appl}(\mathbf{r}_2, t_2)} d(t_1 - t_2), \tag{22}$$

as this can be expressed in terms of the ground- and excited-state wave functions and excitation energies,

$$\chi(\mathbf{r}_1, \mathbf{r}_2; \omega) = \sum_{I \neq 0} \left(\frac{\langle 0|\hat{\rho}(\mathbf{r}_1)|I\rangle\langle I|\hat{\rho}(\mathbf{r}_2)|0\rangle}{\omega - \omega_I + i\eta} - \frac{\langle 0|\hat{\rho}(\mathbf{r}_2)|I\rangle\langle I|\hat{\rho}(\mathbf{r}_1)|0\rangle}{\omega + \omega_I + i\eta} \right), \tag{23}$$

where $\hat{\rho}$ is the density operator and $\eta = 0^+$ is an infinitesimal needed to guarantee causality: $\delta\rho(\mathbf{r}_1, t_1)/\delta v_{appl}(\mathbf{r}_2, t_2) = 0$ if $t_2 > t_1$.

Counterbalancing this marvelous theorem are the representability problems. Given a candidate ground-state charge density that integrates to N electrons, the following questions arise: (*a*) How can we be sure that the density comes from an N-electron wave function (pure-state N representability) or at least from an N-electron ensemble density matrix (ensemble N representability)? (*b*) How can we be sure that it is the ground-state density for some external potential (v representability)? With few exceptions, we find that most reasonable candidate charge densities are pure-state N representable, but determining the v-representability of a candidate charge density is far from obvious.

There is also the problem of how to calculate something nontrivial such as the ground-state energy from a candidate charge density. The second Hohenberg-Kohn theorem solves this problem by using the variational principle to show that $E_0 \leq F[\rho] + \int v_{ext}(\mathbf{r})\rho(\mathbf{r})d\mathbf{r}$, where the functional $F[\rho]$ is universal in the sense that it is independent of the external potential. Equality is achieved for the ground-state charge density. In this case, we can get around the v-representability problem using the Levy-Lieb constrained-search formalism, $F[\rho] = \inf_{\Psi \to \rho}\langle\Psi|\hat{T} + \hat{V}_{ee}|\Psi\rangle$, which says to search over all wave functions (or ensemble density matrices) that produce the trial density. In this sense, the Hohenberg-Kohn functional is not unknown, but it is too complicated to be practical and so approximations must be sought.

Such approximations fall under the category of orbital-free theories, of which Thomas-Fermi theory is the classic historical example. They tend not to be as accurate as approximations based on the Kohn-Sham (re)formulation of DFT. The main problem in making a DFA for an orbital-free theory is finding an approximation for the kinetic energy. The Kohn-Sham formulation of DFT gets around this problem by introducing a fictitious system of noninteracting electrons with the same charge density as the real system of N-interacting electrons. The total energy expression is exactly the same as that in the HF approximation (Equation 3) except that the HF exchange energy, $E_x[\gamma]$, is now replaced with the exchange-correlation (xc) functional, $E_{xc}[\rho]$, and the total electronic energy is exact when the xc-functional is exact (in contrast to HF, which is always an

approximation). Note that the xc-functional, $E_{xc}[\rho] = F[\rho] - E_H[\rho] - \inf_{\Phi\to\rho}\langle\Phi|\hat{T}|\Phi\rangle$, where Φ is a single-determinantal wave function, contains not only the exchange and correlation energies familiar from wave-function theory, but also the difference of the kinetic energies of the interacting and noninteracting systems. Also, before going any further, let us follow modern practice and generalize the original Kohn-Sham DFT to spin DFT so that $E_{xc} = E_{xc}[\rho_\alpha, \rho_\beta]$. Minimizing the total energy with respect to the orthonormal orbitals of the noninteracting system then leads to the Kohn-Sham equation, which differs from the corresponding HF orbital (Equation 1) only by the replacement of the HF exchange self-energy (Equation 2) by the xc-potential,

$$v_{xc}^{\sigma}[\rho_\alpha, \rho_\beta](\mathbf{r}) = \frac{\delta E_{xc}[\rho_\alpha, \rho_\beta]}{\delta\rho_\sigma(\mathbf{r})}. \tag{24}$$

It is now well established that there is a particle number derivative discontinuity (PNDD) in the exact xc-potential, whereby adding a fraction of an electron into a higher-energy orbital leads to a drastic change in the asymptotic behavior of the xc-potential and a nearly rigid shift of the xc-potential in the "bulk region" where the density is large. This may be explicitly verified within the optimized effective potential (OEP) model, which is most easily understood in its classic exchange-only version [often called exact exchange (EXX)]. The EXX model finds the potential whose orbitals minimize the HF energy expression. Alternatively, the EXX potential is that local potential which, upon replacing the HF exchange self-energy, leads to an exactly zero LR of the density. Hence, the EXX and HF densities agree within the LR approximation. Thus, the EXX potential provides an excellent approximation to the true Kohn-Sham x-potential, complete with PNDD. This is easiest to see within the Krieger-Li-Iafrate approximation to the EXX potential for which we now give a heuristic derivation: Let us assume that the HF and KS orbitals are the same on average. If they really were identical, then we could immediately write that $(\hat{\Sigma}_x - v_x(\mathbf{r}))\psi_i(\mathbf{r}) = (\varepsilon_i^{HF} - \varepsilon_i^{KS})\psi_i(\mathbf{r})$. However, this is supposed to be true only on average so we should multiply by $n_i\psi_i^*(\mathbf{r})$ and sum over the index i. After rearrangement, this leads to

$$v_x(\mathbf{r}) = \frac{\sum_i n_i\psi_i^*(\mathbf{r})\hat{\Sigma}_x\psi_i(\mathbf{r})}{\rho(\mathbf{r})} + \frac{\sum_i n_i(\varepsilon_i^{HF} - \varepsilon_i^{KS})|\psi_i(\mathbf{r})|^2}{\rho(\mathbf{r})}. \tag{25}$$

The first term on the right-hand side is Slater's historic definition of the local exchange potential. The second term is the PNDD correction, which is needed because the asymptotic behavior of the charge density depends on the value of highest occupied molecular orbital (HOMO) energy. This second term introduces a rigid shift to compensate for the change in the asymptotic behavior every time a new HOMO is occupied. Such discontinuous behavior is very difficult to incorporate into practical DFAs by anything other than an OEP-like approach.

With the Kohn-Sham formulation, DFT also gains a new representability problem: the noninteracting v-representability (NVR) problem, which requires the presence of an interacting system with integer occupation numbers whose ground state has the same density as that of the interacting system. Violation of NVR appears as a "hole below the Fermi level," meaning that the lowest unoccupied molecular orbital (LUMO) is lower in energy than the HOMO and, thus, in violation of the assumed Fermi statistics for the ground state of the noninteracting system. If we now suppose every system were NVR, then we should always have an exact spin-restricted (SODS) solution for dissociating molecules with a singlet ground state belonging to the totally symmetric representation of the molecular symmetry group. That is, symmetry breaking should never occur for the exact functional because the exact ground-state spin α and spin β densities are identical, implying that $v_{xc}^{\alpha}(\mathbf{r}) = v_{xc}^{\beta}(\mathbf{r})$ and, hence, that the orbitals can always be chosen identically for the different spins (18). However, it now seems likely that not every system is NVR (see Reference 19 and references therein). This leads naturally to fractional occupation numbers, as is easily seen

PNDD: particle number derivative discontinuity

OEP: optimized effective potential

EXX: exact exchange

HOMO: highest occupied molecular orbital

NVR: noninteracting v-representability

LUMO: lowest unoccupied molecular orbital

in the TOTEM. Consider a spin-wave instability, where the Kohn-Sham determinant takes the form $\Psi_\lambda = |\sqrt{1-\lambda^2}\psi_i + i\lambda\psi_a, \sqrt{1-\lambda^2}\bar{\psi}_i + i\lambda\bar{\psi}_a|$, where the absence (presence) of an overbar indicates spin $\alpha(\beta)$. The total energy may then be expanded as $E_\lambda = E_0 + 2\lambda^2(\varepsilon_a - \varepsilon_i) + \mathcal{O}(\lambda^3)$. The spin-wave instability will lower the energy whenever the LUMO energy, ε_i, is lower than the HOMO energy, ε_a (see Reference 20 for a similar example within the HF model). However, it is then easy to demonstrate that the orbitals have a fractional occupation number by looking at the corresponding 1-RDM operators,

Pure density functional: depends only on the density, excluding any orbital dependence

$$\begin{aligned}
\hat{\gamma}_\alpha &= (1-\lambda^2)|i\rangle\langle i| + i\lambda\sqrt{1-\lambda^2}(|a\rangle\langle i| - |i\rangle\langle a|) + \lambda^2|a\rangle\langle a| \\
\hat{\gamma}_\beta &= (1-\lambda^2)|i\rangle\langle i| - i\lambda\sqrt{1-\lambda^2}(|a\rangle\langle i| - |i\rangle\langle a|) + \lambda^2|a\rangle\langle a| \\
\hat{\gamma} &= \hat{\gamma}_\alpha + \hat{\gamma}_\beta = 2(1-\lambda^2)|i\rangle\langle i| + 2\lambda^2|a\rangle\langle a|.
\end{aligned} \tag{26}$$

These observations are consistent with the traditional assumption that an ensemble formalism with fractional occupation number is needed in cases where NVR fails. An important theorem in this context is that all fractionally occupied orbitals must be degenerate with lower-energy orbitals that are fully occupied and higher-energy orbitals that are completely vacant (see, e.g., Reference 17, pp. 55–56). Surprisingly, there is some indication that the noninteracting system may become degenerate in such a theory for a range of molecular configurations where the interacting system is nondegenerate (21). One is then faced with the potential problem of minimizing the energy with respect to unitary transformations within the space spanned by the degenerate occupied orbitals with different occupation numbers.

3.2. Approximations

DFT is hardly useful without DFAs. Perdew has organized functionals into a type of Jacob's ladder (**Figure 3**). The basic idea is that gradually including more information about the local density, the reduced gradient, the local kinetic energy, etc., allows users (angels going up the ladder) the added flexibility needed to create more accurate functionals. Only the first two rungs (or three if the local kinetic energy is excluded from the third rung) constitute pure density functionals—that is, functionals that stick to the original spirit of Hohenberg-Kohn-Sham DFT and consider only the density as the working variable. For this reason it may be better to refer to the higher rungs as generalized Kohn-Sham. It must be emphasized that, although greater accuracy is not guaranteed, there is a general tendency toward more accurate functionals when going to higher rungs of the ladder. However, it is important that users also be able to descend the ladder when necessary, as calculations necessarily become more complex and expensive on the higher rungs of the ladder.

One of us has generalized Jacob's ladder to "Jacob's jungle gym" (22) by including additional ladders corresponding to higher xc-derivatives. For pure density functionals, these would be defined by Equation 24 and

$$\begin{aligned}
f_{xc}^{\sigma_1,\sigma_2}(\mathbf{r}_1,\mathbf{r}_2) &= \frac{\delta^2 E_{xc}[\rho_\alpha,\rho_\beta]}{\delta\rho_{\sigma_1}(\mathbf{r}_1)\delta\rho_{\sigma_2}(\mathbf{r}_2)} \\
g_{xc}^{\sigma_1,\sigma_2,\sigma_3}(\mathbf{r}_1,\mathbf{r}_2,\mathbf{r}_3) &= \frac{\delta^3 E_{xc}[\rho_\alpha,\rho_\beta]}{\delta\rho_{\sigma_1}(\mathbf{r}_1)\delta\rho_{\sigma_2}(\mathbf{r}_2)\delta\rho_{\sigma_3}(\mathbf{r}_3)},
\end{aligned} \tag{27}$$

where the xc-kernel f_{xc} and xc-hyperkernel g_{xc} are needed for static-response properties. Analogous quantities are found at each of the higher rungs. This type of representation is useful because derivative quantities are always harder to approximate than the quantities whose derivative is being taken. Thus, combining different approximations from different ladders may be appropriate when calculating certain types of quantities.

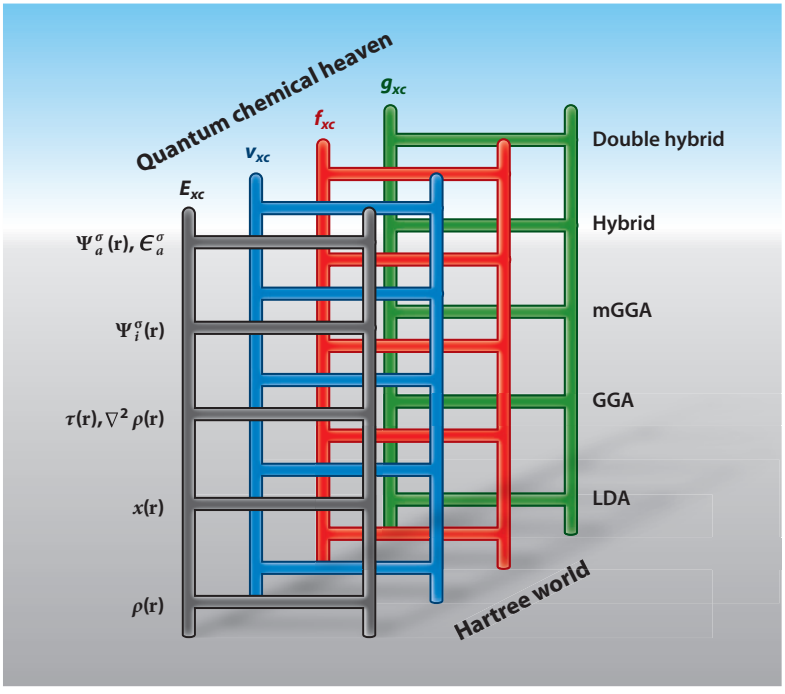

Figure 3

The front (*gray*) ladder of "Jacob's jungle gym" (22) represents the Jacob's ladder for E_{xc} (23). Spin indices have been dropped for simplicity; however, present practice is to use spin-density functional theory wherever the density is a two-component object, $(\rho_\alpha, \rho_\beta)$. The local density approximation (LDA) involves only the density $\rho(\mathbf{r})$ at each point; the generalized gradient approximation (GGA) involves both $\rho(\mathbf{r})$ and the reduced gradient $x(\mathbf{r}) = |\vec{\nabla}\rho(\mathbf{r})|/\rho^{4/3}(\mathbf{r})$; the meta (m)GGA involves $\rho(\mathbf{r})$, $x(\mathbf{r})$, and the local kinetic energy $\tau(\mathbf{r}) = \Sigma_p n_p \psi_p(\mathbf{r})\nabla^2\psi_p(\mathbf{r})$ or the Laplacian of the density, $\nabla^2\rho(\mathbf{r})$. The fourth rung involves hybrid functionals, exact exchange, and related functionals. There, explicit information about occupied orbitals is also incorporated into the functional. On the fifth and highest rung, we encounter double hybrids, functionals based on the adiabatic connection fluctuation-dissipation theorem, and related functionals. At this highest level, explicit information is added about unoccupied orbitals and their orbital energies, and the DFA closely approaches conventional many-body perturbation theory.

3.3. Scale-Up

Because the Kohn-Sham DFT resembles the HF approximation, which is the basis of much of the development of (non-DFT) ab initio quantum chemistry, comparing the two approaches is relatively easy, as is incorporating a Kohn-Sham solver into a wave-function ab initio approach. This makes especially good sense if DFAs are viewed as a way of extending the accuracy of wave-function ab initio approaches to systems larger than would otherwise be possible. In this sense, the problem of how to scale-up calculations is highly relevant to the success of DFT and DFAs. Owing to space limitations, however, we say only a few words about scale-up strategies.

The lower rungs of Jacob's ladder (i.e., the LDA and the GGAs) have long been noted to resemble the Hartree more closely than the HF approach. As such, rather than the formally $\mathcal{O}^{(4)}(N)$ scaling of the HF approach, the introduction of density-fitting functions leads to a formal $\mathcal{O}^{(3)}(N)$ scaling, which is further improved by integral prescreening. Beyond a certain system size (i.e., once a certain level of computational power is reached), special algorithms such as those that scale asymptotically as $\mathcal{O}(N)$ can be used. These algorithms are especially easy to apply in the case

of DFT, and they make linear-scaling DFT extremely attractive for large-scale "chemistry on the computer" (24).

DFTB: density-functional tight binding

ΔSCF: method consisting of calculating the energy difference of two SCF calculations

A second scale-up strategy is the subsystem approach where formal DFT (25, 26) is extended to describe subsystems of larger systems: for example, molecules hydrogen bonded to other molecules, molecules in solution, or fragments of molecules covalently bonded to the whole. Corresponding DFAs can then be developed. By allowing a Kohn-Sham description of a subsystem to be embedded within a larger surrounding system described using an orbital-free DFA, such an approach is able to treat larger systems. This subsystem approach is also attractive from an interpretational point of view as it corresponds well with the idea of functional groups in organic chemistry and active sites in biochemistry. An intriguing development is the successful implementation of subsystem DFT for cases when the subsystem is covalently bonded to the larger system (27, 28).

A final strategy is the development of the density-functional tight-binding (DFTB) model with parameters obtained from Kohn-Sham calculations (29). Although it loses some of the rigor of a true Kohn-Sham calculation, DFTB is a next logical step in a multiscale strategy to larger spatial and temporal scales than can normally be obtained by true Kohn-Sham calculations.

4. TIME-DEPENDENT DENSITY-FUNCTIONAL THEORY

The classic Hohenberg-Kohn-Sham DFT considers the ground stationary state. However, as mentioned in Section 1, chemistry is not just a matter of the ground stationary state, but also of UV-visible spectroscopy, nonlinear optics, photochemistry, and other applications involving either TD electronic properties and/or electronic excited states.

In 1999, Singh & Deb (30) reviewed the prospects for treating excited states within a DFT framework. Up to 1995 (4), the most popular method was the ΔSCF approach and its MSM variant. Because the classic Hohenberg-Kohn-Sham DFT can handle electronic ground states, it is possible to carry out SCF calculations for the ground states of a neutral molecule, its anion, and its cation. Taking energy differences yields a rigorous method for calculating the first ionization potential and electron affinity, and adding or removing electrons from other orbitals provides an ad hoc way to estimate other ionization potentials and electron affinities. For some of these ionization potentials and electron affinities, the method may be considered to be reasonably rigorous so long as we accept that the DFAs developed for the true ground states also apply to the ground state of each symmetry, particularly if a single determinant is a reasonable first approximation. Within the same assumption, the lowest triplet excitation energy of a closed-shell molecule may also be calculated reasonably rigorously within the ΔSCF method. For open-shell singlet excited states, Ziegler et al. (12) and Daul (30a) adapted the MSM as an excited-state DFA. The result in the TOTEM is given in **Table 1** after linearization. Minus the ionization potential, I_i, of orbital i and minus the electron affinity, $A_a(i^{-1})$, are given by expressions very different than those given by Koopmans' theorem. In fact, contra the HF case, Kohn-Sham orbitals should be preprepared to describe excitations given that, for pure DFAs, the occupied and unoccupied orbitals "see" the same potential and, hence, the same number of electrons. This is particularly clear in the expression for the mixed-state excitation energy, ω_M, which is a simple orbital energy difference when the densities of the initial (i) and final (a) orbitals are the same. The additional term is a correction for relaxation of the orbital densities during the excitation process. Thus, much quality physics is present in the MSM DFA for excited states. However, the need to estimate the form of the excited-state wave function typically on the basis of symmetry arguments presents a major difficulty with this method. Thus, only a first-order estimate may be obtained in many cases, and automating for excited-state calculations becomes more difficult than within TD-DFT.

4.1. Classic TD-DFT

A new question arises: To what extent can the time evolution of the charge density be treated without having to solve the full TD Schrödinger equation,

$$\hat{H}(t)\Psi(t) = i\frac{\partial}{\partial t}\Psi(t), \tag{28}$$

for the N-electron wave function, $\Psi(t) = \Psi(1, 2, \ldots, N, t)$? Before discussing this question, recall that the TD problem is an initial value problem: Given $\Psi_0 = \Psi(t_0)$, propagate the wave function forward in time to obtain $\Psi(t)$. Thus, the wave function at time t is a functional of the wave function at time t_0, $\Psi[\Psi_0](t)$.

Because the TD N-electron Schrödinger equation can rarely be solved exactly, approximate solutions are often sought. This is typically done using the Frenkel-Dirac stationary action principle (32–34), which implies that the TD Schrödinger equation is satisfied over the time interval (t_0, t) when the action,

$$A[\Psi; \Psi_0](t, t_0) = \int_{t_0}^{t} \left(\langle \Psi[\Psi_0](t')| i\frac{\partial}{\partial t'} |\Psi[\Psi_0](t')\rangle - E[\Psi_0](t') \right) dt', \tag{29}$$

is made stationary with respect to variations of $\Psi[\Psi_0](t')$ on the interval $t' \in (t_0, t)$ and subject to the constraints $\delta\Psi[\Psi_0](t_0) = \delta\Psi[\Psi_0](t) = 0$. Here,

$$E[\Psi_0](t) = \langle \Psi[\Psi_0](t)|\hat{H}|\Psi[\Psi_0](t)\rangle \tag{30}$$

is the "instantaneous energy," which can, in principle, also contain information about system dynamics from previous times. Such an understanding emphasizes the main point of this stationary action principle: An approximate equation of motion may be developed from any approximate instantaneous energy expression. Finding a problem with the original Frenkel-Dirac principle, Vignale (35) noted that $\delta\Psi[\Psi_0](t) = 0$ cannot be freely set because causality requires that the boundary condition Ψ_0 determine $\Psi[\Psi_0](t)$. When this is taken into account, the new Frenkel-Dirac-Vignale stationary action principle (35) becomes

$$\delta A[\Psi; \Psi_0](t, t_0) = i\langle \Psi[\Psi_0](t)|\delta\Psi[\Psi_0](t)\rangle, \tag{31}$$

which is subject only to the obvious constraint that $\delta\Psi[\Psi_0](t_0) = 0$ implies that the TD Schrödinger equation be satisfied over the time interval (t_0, t). Note that the right-hand side of Equation 31 is set to zero in the original Frenkel-Dirac formulation. Despite this difference, the two stationary action principles often give the same result (35), which is fortunate because the Vignale correction is rarely invoked. Note also that Lagrange multipliers may be easily added to apply the constraints frequently needed when deriving equations within a given model.

Now let us return to the question of the extent to which the TD wave function may be replaced by the TD charge density. It is natural to replace the instantaneous energy in the Frenkel-Dirac action with the Kohn-Sham energy and the wave function with the Kohn-Sham determinant. The Frenkel-Dirac stationarity condition then leads to the TD Kohn-Sham equation,

$$\left[-\frac{1}{2}\nabla^2 + v_{ext}(t) + v_H[\rho(t)] + v_{xc}[\rho_\alpha(t), \rho_\beta(t)] \right] \psi_i(t) = i\frac{\partial \psi_i(t)}{\partial t}. \tag{32}$$

Although this equation was used as early as 1980 (36) to calculate photoabsorption cross sections of rare gas atoms, researchers did not establish the formal justification until later.

Formal TD-DFT is usually traced back to the classic paper of Runge & Gross (3), which tried to firm up earlier work on the same subject. Thus, the Runge-Gross TD-DFT is two decades younger than its stationary ground-state older sibling, the Hohenberg-Kohn-Sham theory. The Runge-Gross paper contains four theorems. The first is the Runge-Gross theorem, which states that the

CDFT: current density-functional theory

TD charge density, $\rho(\mathbf{r}, t)$, together with the initial wave function, Ψ_0, determine the external potential up to an additive function of time. This implies that the wave function is determined up to an arbitrary phase factor, $\Psi(t) = e^{-i\phi(t)}\Psi[\rho, \Psi]$. The proof proceeds in two steps: First, any Taylor-expandable TD external potential is determined by Ψ_0 and by the current density, $\mathbf{j}(\mathbf{r}, t)$. Second, $\rho(\mathbf{r}, t)$ is determined by $\mathbf{j}(\mathbf{r}, t)$. Xu & Dhara (37) noted a weakness in the second step of the proof, but it can be excluded for physically reasonable external potentials that may be viewed as being made up of point charges (38, 39). Although the TD-DFT community is very self-critical, the proof of this theorem has withstood the test of time. The second theorem in the Runge-Gross paper proposes a hydrodynamical formulation of TD-DFT. The third theorem proposes making the Frenkel-Dirac action the basis for a variational theorem analogous to the second Hohenberg-Kohn theorem. Unfortunately, this theorem is wrong as stated because (as is always the case with the Frenkel-Dirac principle) it does not handle causality correctly. Many subsequent reformulations of the action have been proposed including one by Rajagopal involving the Berry phase (40), formulations involving the Keldysh action (41, 42), and Liouville space pathways (43). However, the use of the Frenkel-Dirac-Vignale action (35) seems to be by far the simplest solution. The fourth theorem in the Runge-Gross paper proposes a Kohn-Sham formulation of TD-DFT, which clarifies the nature of the TD xc-potential. Whether written as the derivative of an xc-action,

$$v_{xc}^{\sigma}[\rho_\alpha, \rho_\beta; \Psi_0, \Phi_0](\mathbf{r}, t) = \frac{\delta A_{xc}[\rho_\alpha, \rho_\beta; \Psi_0, \Phi_0]}{\delta\rho_\sigma(\mathbf{r}, t)}, \tag{33}$$

or simply postulated to exist, the xc-potential in TD Kohn-Sham theory has a formal dependence on the initial wave functions of the real interacting Ψ_0 and noninteracting Kohn-Sham Φ_0 systems of N-electrons. This initial-state dependence may be "eliminated" using the first Hohenberg-Kohn theorem if the initial state of the system is the ground stationary state (e.g., Ψ_0 and Φ_0 are determined by ρ at t_0). Even so, we do not recover the xc-potential of Equation 32, where time is considered to be a parameter and the derivative is taken at fixed time. As a local approximation in time, this important AA of TD-DFT assumes that the xc-potential reacts instantaneously and without memory to any temporal change in the charge density. The exact TD-DFT xc-potential should have memory in the sense of depending on the past history of the charge density, making it a functional of a function of not just $(\mathbf{r}, \sigma)$ but also of t. The AA may be taken as the definition of conventional TD-DFT and, in practical terms, predates the Runge-Gross paper. The challenge now presented by Runge and Gross is to determine how memory effects are included in a TD xc-functional.

The Runge-Gross formulation of TD-DFT is limited to applied electric fields. This is sufficient for many problems because magnetic field effects are often significantly smaller than electric field effects in experimental studies of molecular properties, but it would be better to have a gauge-invariant theory that treats electric and magnetic fields equally. Ghosh & Dhara (44) extended TD-DFT to handle TD magnetic fields by introducing a current-density dependence and an exchange-correlation vector potential. TD current DFT (CDFT) has since developed considerably (for a recent paper on this topic, see Reference 45). Alternatively, calculations may be formulated and carried out within the framework of 4-component relativistic TD-DFT (46).

4.2. Applications

In the quarter century since the publication of the Runge-Gross paper (3) and the introduction of TD-DFT into quantum chemistry over a decade ago (4), there have been several interesting applications of this theory. We highlight a few here that we find especially interesting.

4.2.1. Absorption spectra. The major application of TD-DFT is to calculate electronic absorption spectra using LR theory. In Section 3.1, we argue that the first Hohenberg-Kohn theorem guarantees that the dynamic LR of a system of N-electrons is determined by the ground-state charge density, but we had no practical way to construct this response. TD-DFT provides such a procedure through the dynamic LR of the charge density. The calculation consists of propagating the Kohn-Sham orbitals in the presence of a small dynamic perturbation, $v_{appl}(\mathbf{r}, t) = \mathcal{E}(t) \cdot \mathbf{r}$, and calculating the induced dipole moment, $\mu_{ind}(t)$, which is the difference between the TD and permanent dipole moments of the system. The dynamic polarizability α is defined by the linear term $\mu_{ind}(t) = \int \alpha(t - t')\mathcal{E}(t')dt'$. Applying the Fourier transform convolution theorem allows us to calculate the dynamic polarizability as $\alpha(\omega) = \mu(\omega)/\mathcal{E}(\omega)$. Because the dynamic polarizability has the sum-over-states form,

$$\alpha(\omega) = \sum_{I \neq 0} \frac{f_I}{\omega_I^2 - \omega^2}, \tag{34}$$

where ω_I and f_I are vertical excitation energies and the corresponding oscillator strength, respectively. Thus, the Laurentzian broadened stick spectrum can be obtained as

$$\mathcal{S}(\omega) = \frac{2\omega}{\pi} \Im m\, \alpha(\omega + i\eta). \tag{35}$$

Such a procedure has been implemented, for example, in the Octopus code (47), and it has the advantage of calculating the absorption spectrum of a very large molecule over a wide range of energies, albeit with only moderate spectral resolution.

Taking a different approach, one of us (4) showed how LR-TD-DFT could be formulated through an analytic treatment of the poles of the dynamic polarizability to look like the RPA equation (Equation 8), thus allowing a rapid implementation of TD-DFT in ab initio quantum chemistry wave-function codes. This method is now found in nearly every internationally important quantum chemistry and quantum physics code. The derivation of Reference 4 did not make the AA and allowed for (fixed) fractional occupation numbers. The matrices **A** and **B** are ω-dependent in the general theory, and the number of solutions exceeds the dimensionality of the matrix problem. However, for brevity, we write only the matrix elements of the **A** and **B** matrices here in the AA:

$$\begin{aligned} A_{ia\sigma,jb\tau} &= \delta_{\sigma,\tau}\delta_{i,j}\delta_{a,b}(\varepsilon_{a\sigma} - \varepsilon_{i\sigma}) + (ia|f_H + f_{xc}^{\sigma,\tau}|bj) \\ B_{ia\sigma,bj\tau} &= (ia|f_H + f_{xc}^{\sigma,\tau}|jb). \end{aligned} \tag{36}$$

Once LR-TD-DFT equations are formulated for TD-DFT, the TDA may be used, yielding an approximation that was introduced into the TD-DFT literature by Hirata & Head-Gordon (48). Just as the variational nature of CIS is helpful in circumventing, or at least, reducing problems associated with triplet and near-singlet instabilities in the HF RPA, so too is the TDA highly useful when calculating TD-DFT excited-state PESs (13, 18, 19). However, the cost of the TDA is a loss of oscillator strength sum rules (49) with possible implications for the accuracy of corresponding spectra (50).

Turning our attention to the TOTEM, we now say a few words about why TD-DFT works from a physical point of view. At least on the lower rungs of Jacob's ladder (LDA and GGAs), the Kohn-Sham orbitals are preprepared to describe electronic excitations given that the occupied and unoccupied orbitals "see" the same xc-potential and, hence, the same number of electrons. Thus, except for charge-transfer excitations, which have large amounts of density relaxation, the TOTEM often applies fairly well in TD-DFT. The corresponding TDA TD-DFT singlet and triplet excitation energies are given in **Table 1**. An examination of the size of the various integrals

then shows that

$$\omega_T < \varepsilon_a - \varepsilon_i < \omega_S, \tag{37}$$

with all three values becoming identical for Rydberg states where the differential overlap $\psi_i(\mathbf{r})\psi_a(\mathbf{r})$ becomes negligible. At lower energies, we should expect to recover the STEX formulae. As shown in **Table 1**, this is possible, at least roughly, within a sufficiently accurate model such as the OEP model (14). Direct calculation shows that the Koopmans' theorem interpretation of the occupied orbital energies as the negatives of ionization potentials holds better than it does for HF. Thus, $I_i = \varepsilon_i$. However, the energies of the unoccupied orbitals do not represent the negatives of electron affinities because the occupied orbitals "see" $N-1$ rather than N electrons. The quantity $A_a(i^{-1})$ is minus the electron affinity of the orbital ψ_a for the cation with an electron removed from orbital ψ_i. The electron, thus, "sees" $N-1$ electrons, so $A_a(i^{-1})$ is to a first approximation equal to ε_a of the N-electron neutral. However, one Hartree and one exchange interaction with the electron in orbital ψ_i have been removed, so we now have to update the approximation to read $A_a(i^{-1}) = \varepsilon_a + (ai|f_H + f_{xc}^{\alpha,\alpha}|ia)$. [Note that the Hartree interaction is estimated in TD-DFT by the integral $(ai|f_{xc}^{\alpha,\alpha}|ia)$.]

4.2.2. Photochemistry. The popularity of TD-DFT for modeling absorption spectra is a strong incitation to extend TD-DFT to the related photophenomena shown in **Figure 1**. We are immediately confronted with the fact that TD-DFT provides only excitation energies, $\omega_I = E_I + E_0$, so that excited-state PESs must be calculated by adding the excitation energy obtained from TD-DFT to the ground-state energy obtained by static ground-state DFT: $E_I^{TD-DFT} \equiv E_0^{DFT} + \omega_I^{TD-DFT}$. Exploring excited-state PESs is facilitated by the implementation of analytic gradients for TD-DFT excited states, $\nabla E_I^{TD-DFT} = \nabla E_0^{DFT} + \nabla \omega_I^{TD-DFT}$, in many electronic structure codes.

The first and easiest of these phenomena that can be treated is fluorescence. The TD-DFT fluorescence energy is a TD-DFT singlet excitation energy calculated at the optimized geometry of the singlet excited state. The corresponding Stokes shift is the difference between the absorption and fluorescence energies: $\omega_{STOKES} = \omega_{ABS} - \omega_{FLUO}$.

More challenging is to use TD-DFT to investigate possible photochemical reaction mechanisms. Although TD-DFT is a well-established part of the photochemical modelers' toolbox, applications to study the entire course of a photochemical reaction are relatively new. The reader is referred to a recent review on the subject by Casida et al. (51). It is now increasingly possible to go beyond Ehrenfest dynamics or the simple pathway method and carry out mixed TD-DFT/classical trajectory surface-hopping calculations to get an idea of potential photochemical reaction mechanisms and reaction branching ratios (19, 52–54).

4.2.3. The challenge of excitonics. To judge by the numerous articles that have appeared in the *Annual Review of Physical Chemistry*, excitonics (or the study of excitons) is of great and recurring interest to our community. It would most likely be described differently by a solid-state physicist and by a physical chemist or biophysicist. A solid-state physicist would probably begin with the image of delocalized states with the expected broad-absorption spectra. Sharp spectral features are then often associated with localized excitations that could propagate throughout a material and eventually the electrons and holes could separate to do something interesting such as generate electricity or drive a chemical reaction. A physical chemist or biophysicist would probably begin by dissecting an extended system, such as a molecular solid or a biomolecule, into components that are likely to have localized excitations and then use an excitonic model to try to understand how excitations interact to lead to spectral shifts or energy transfer. In the end, the concepts are

not very different, except that the solid-state physicist is localizing a delocalized phenomenon, whereas the chemist is delocalizing localized phenomena.

These two points of view are now frequently coming together in the area of nanoscience where solids and molecules meet at the nanointerface. This is particularly apparent when modeling dye-sensitized solar cells (55). A level-matching problem exists in systems where the excited states of dye molecules must be aligned with the band structure of transparent semiconductor particles, for example, so that electrons can pass into the conduction band when neutral excitations break up at the molecule-crystal interface. Calculations such as that in Reference 56 give an idea of what is currently possible when modeling dye-sensitized solar cells with TD-DFT.

Excitons are also highly relevant in photobiology where excitations in nearby proteins are coupled, thus allowing energy to be captured by antenna systems and transported to active sites where electronic energy is used to do biologically important chemistry. Both for practical and conceptual reasons, it makes sense to use subsystem DFT. By implementing and improving the subsystem version of TD-DFT initially proposed by Casida & Wesołowski (27), Neugebauer (57, 58) has been particularly successful in this regard. This theory has also been recently applied to the light-harvesting complex II of green plants (59). Given the system sizes involved and the importance of simulating exciton dynamics, TD-DFT will have to be combined with semiempirical models, such as TD-DFTB (60), to describe the full complexity of excitonic phenomena.

4.3. Problems, Problem Detection, and Solutions

By discussing the applications of TD-DFT before discussing the problems of TD-DFT, we may have given the false impression that classical TD-DFT is a fail-safe method. It is far from that! Just as pure Kohn-Sham DFT looks like the HF (or rather the Hartree) approximation but behaves very differently, TD-DFT, even if put in the form of the classic RPA equation of quantum chemistry, does not behave like TD-HF. Conventional LR-TD-DFT in its basic AA using pure DFAs often, but not always, works better than LR-TD-HF. It works best for (*a*) low-energy, (*b*) one-electron excitations involving (*c*) little or no charge transfer and (*d*) that are not too delocalized. This section examines the reasons for these limitations and gives a few suggestions as to what can be done when a better solution is needed. Interestingly, many of the problems are not due to the AA, so that our analysis may be carried out in terms of Jacob's jungle gym (**Figure 3**). Discussion of problems associated with the AA and possible solutions is delayed till Sections 5 and 6.

4.3.1. Problems associated with E_{xc}. There is an intimate relationship between the ground- and excited-electronic states in conventional TD-DFT. Not only are the excited-state PESs obtained by adding TD-DFT excitation energies to the DFT ground-state energy, but the same **A** and **B** matrices that occur in LR-TD-DFT also occur in a stability analysis of the DFT ground state (13, 22, 61). In fact, the theory closely parallels what happens in HF stability analysis (Section 2.3).

To understand the similarities and differences between what happens in DFT and HF, let us first look at the classic example of H_2. In HF theory, stretching the bond beyond the Coulson-Fischer point leads to symmetry breaking such that a DODS solution becomes lower in energy than an SODS. The presence of ionic contributions in the DODS HF wave function produces this result, which is well understood in wave-function theory. The situation is different in DFT. Assuming NVR, we must have an SODS solution. A unique nodeless orbital, $\psi(\mathbf{r})$, is found by taking the square root of the density. The noninteracting potential is then calculated as $v_s(\mathbf{r}) = (\nabla^2\psi(\mathbf{r})/2\psi(\mathbf{r})) - \varepsilon$, with the orbital energy, ε, adjusted so that v_s goes to zero at infinity. The NVR assumption may then be explicitly verified by solving the Kohn-Sham equation to make sure that ε corresponds to the lowest orbital energy of the noninteracting system. In this way, symmetry breaking does not occur in the exact theory.

RDMFT: reduced density-matrix functional theory

But symmetry breaking does occur for DFAs, even though it is not as severe as in HF. In particular, the Coulson-Fischer point for pure density functionals occurs at larger H_2 bond distances than in HF, but it does occur and is recognizable because the square of the lowest triplet excitation energy, ω_T^2, goes to zero exactly at the Coulson-Fischer point before becoming negative (an imaginary triplet excitation energy) at larger distances (13). Incidentally, an SCF calculation may begin with an SODS guess to converge to an SODS solution even when there is a lower-energy DODS solution (62). In this sense, a TD-DFT calculation may serve as an important check on the correctness of the ground-state calculation. However, when the goal is to calculate excited-state PESs, the presence of triplet and near-singlet instabilities is highly inconvenient. As in the HF case, a partial solution is provided by the TDA whose excitation energies "inherit" some of the variational nature of CIS and so do not collapse when the ground-state solution becomes unstable (13, 18, 19).

A second phenomenon that can occur when breaking a bond is the occurrence of a cusp in the ground-state PES when orbital fillings suddenly change (18, 63). The wave-function solution to this problem is to allow configurations to mix, allowing the wave function to be a linear combination of determinants corresponding to the two different orbital fillings. By contrast in DFT calculations, such an outcome usually corresponds to the situation of effective failure of NVR when the LUMO falls lower in energy than the HOMO. Because most DFT programs enforce Aufbau filling of the orbitals, the LUMO is immediately filled so that it becomes the next HOMO and the old HOMO becomes the new LUMO. However, the LUMO remains lower than the HOMO and the calculation simply fails to converge (18, 19). As discussed in Section 3.1, this "strange" orbital filling means that we are in the presence of a spin-wave instability. The conventional DFT solution moves to ensemble theory and allows the orbitals to have a fractional occupation number. Unfortunately, it remains unclear how well conventional DFAs apply to the ensemble situation.

This situation is probably one of the contributing factors prompting the development of reduced density-matrix functional theory (RDMFT). In principle, the density is replaced with the 1-RDM. However, in practice, the natural orbitals and their corresponding occupation numbers become the fundamental variables. As such, RDMFT highly resembles ensemble density functional theory but also has the possibility of handling nonlocal potentials (i.e., one-electron operators that are not simply multiplicative functions). Exact equations may also be derived for two-electron systems, as Löwdin & Shull (64) showed that the two-electron wave function may be expanded exactly. The spatial part is given by

$$\Psi(\mathbf{r}_1, \mathbf{r}_2) = \sum_i \sqrt{\frac{n_i}{2}} e^{i2\alpha_i} \phi_i(\mathbf{r}_1)\phi_i(\mathbf{r}_2), \tag{38}$$

where the natural orbitals $\phi_i(\mathbf{r})$ are assumed to be real, their complex phase α_i has been exhibited explicitly, and the associated natural orbital occupation numbers are denoted by n_i. Defining the phase is the major problem in the two-electron theory, but the minority natural orbitals are usually found empirically to have a negative phase with respect to the dominant phase. Very good exact functionals may then be developed for the two-electron case, which gives the correct dissociation of H_2. For notable early work attempting to develop 1-RDM functionals for systems with more than two electrons, see Müller (65) and Goedecker & Umrigar (66). For more recent work, see Reference 67 and references therein.

Finally, a problem with conical intersections arises precisely because excited-state PESs are calculated in TD-DFT as $E_I = E_0 + \omega_I$. For a molecule with N_f internal degrees of freedom, $\mathbf{Q}$, the PES is an N_f-dimensional object in an $(N_f + 1)$-dimensional space (because we have added the energy axis). When two PESs cross, we have two constraints: (*a*) $E_I(\mathbf{Q}) = E_J(\mathbf{Q})$ and (*b*) $H_{I,J}(\mathbf{Q}) = 0$. The first constraint is always present in TD-DFT and reduces the dimensionality

of the crossing space to a hyperline always. The second constraint should further reduce the dimensionality of the intersection space to a hyperpoint, i.e., a conical intersection where there are two independent directions going away from the intersection space in hyperspace where the surfaces separate (unless we have a diatomic so that $N_f = 1$, in which case, an avoided crossing is present). However, Levine et al. (68) have noted that the second constraint is absent for interactions between the excited states and the ground state because of the use of the formula $E_I = E_0 + \omega_I$. We are thus left with the condition that conical intersections cannot exist in TD-DFT. Nevertheless, in practice, conical intersections may be approached closely enough to make mixed TD-DFT/classical surface-hopping photodynamics calculations qualitatively useful for investigating photochemical reaction mechanisms (19).

4.3.2. Problems associated with v_{xc}. In terms of E_{xc}, problems typically arise at the molecular geometries corresponding to bond making or breaking in the ground state. Problems associated with v_{xc} also occur in the Franck-Condon region near the ground-state equilibrium geometry. In Section 4.1, we argue that the Kohn-Sham orbital energy difference should lie between the corresponding singlet and triplet excitation energies (Equation 37) and that all three quantities will be well approximated by the Kohn-Sham orbital energy difference for Rydberg-type excitations. Because the limit of a given Rydberg series is the ionization potential of an orbital ψ_i, we see immediately that the TD-DFT ionization threshold is at minus the HOMO energy. However, practical DFAs have minus HOMO energies that are typically several electron volts too low compared with the experimental ionization potential. As a result, finite-basis TD-DFT calculations lead to a collapse of the higher excited states in the region between minus the HOMO energy and the true ionization potential (69). The reader needs to be keenly aware of this point because the collapse may not be obvious when only medium-sized basis sets are used, though it will occur once larger-sized basis sets are employed.

One approach to this problem is to ignore it. After all, the oscillator strength distribution should be approximately correct even above the TDLDA ionization threshold at $-\varepsilon_{HOMO}$ (70). However, transitions to bound states will no longer be sharp, making assignments more difficult, but the spectral features are often still present.

A better approach may be to correct the asymptotic behavior of v_{xc} by a shift-and-splice approach (see Reference 71 and references therein). This is sufficient, to obtain qualitatively reasonable Rydberg PESs and, hence, to see valence-Rydberg avoided crossings in TD-DFT calculations for formaldehyde ($H_2C = O$) (72). An even more sophisticated approach is the OEP model (see above).

A subtler issue discussed only occasionally in the DFT literature is that the relative orbital energies of occupied orbital energies obtained with DFAs may not be correct compared with the orbital energies that should come out of exact Kohn-Sham DFT calculations. In References 22 and 73, OEP calculations were used to show that errors in ethylene ($H_2C = CH_2$) asymptotically corrected LDA TD-DFT excitation energies were due to small relative errors in the occupied σ and π MO energies.

Charge-transfer excitations present another significant problem (74). Up to this point, we have argued that DFT orbitals are preprepared to describe excitations, but a better statement is that they are preprepared to describe neutral excitations. As discussed in Section 2.2, HF theory is well designed for describing long-range charge transfer. An inspection of the TDA-TD-TDDFT formulae in **Table 1** shows that the long-range charge-transfer energy in TD-DFT is the orbital energy difference, $\varepsilon_a - \varepsilon_i$, which is badly underestimated because of problems with the asymptotic behavior of v_{xc} related to the PNDD. This also suggests that the overlap between the initial and final orbitals in an excitation could be used as a diagnostic tool to anticipate when TD-DFT will

break down due to charge-transfer excitations (75). As the linearized ΔSCF DFT formulae in **Table 1** show, this problem is not as severe in the ΔSCF approach, which takes partial account of orbital relaxation energies, making it the basis of one proposal for a charge-transfer correction (13). Casida et al. (13) add that only the charge-transfer excitations involving density relaxation are problematic in TD-DFT. In fact, Mulliken's prototypical $^1\Sigma_u$ charge-transfer excitation in H_2 is an excellent example where density relaxation is small and TD-DFT has few problems. However, a better answer can be found in the range-separated-hybrid approach (see Reference 76 and references therein, where the electron repulsion, $1/r_{12}$, is separated into a short-ranged part described by a pure DFA, $(1/r_{12})_{SR} = \mathrm{erfc}(\gamma r_{12})/r_{12}$, and a long-range part described by a suitable wave-function theory such as HF, $(1/r_{12})_{LR} = \mathrm{erf}(\gamma r_{12})/r_{12}$. There are several variations on the name and precise functional forms used in this theory, but they all yield a dramatic reduction in errors due to the underestimation of charge-transfer excitations. A drawback is the potential presence of a system-dependent parameter (γ in the above example).

Interestingly, a recent OEP study shows that errors in the charge-transfer excitation of HeH^+ are not due to errors in the xc-kernel, but rather to errors in Kohn-Sham orbital energies arising from DFAs (77). A second OEP study confirms that a significant part of the errors in the adiabatic TD-DFT is due to the use of DFAs, but it goes on to show that an important residual error is due to neglect of the frequency dependence of the xc-kernel (78).

4.3.3. Problems associated with f_{xc}. There are two main problems associated with f_{xc}. First is the need to include, not just 1p1h excitations, but also higher excitations to treat some problems. For example, explicit 2p2h excitations are needed to describe the first singlet excited state of butadiene, $CH_2 = CHCH = CH_2$, which has significant double-excitation character (79). Furthermore, explicit higher-electron excitations are needed for a proper description of excitations of molecules with open-shell ground states (80). Although exact TD-DFT should describe this correctly, making the AA restricts the number of solutions of the LR-TD-DFT equation to the dimensionality of the matrix, namely only the number of 1p1h excitations and de-excitations. Including some frequency dependence in f_{xc} could allow a nonlinear feedback mechanism allowing the matrix equation to have additional solutions. By going beyond LR to look at simultaneous two-photon absorption, for example, researchers had hoped two-electron excitations could be treated within the AA (81); however, it is now clear that this is not the case. In particular, the poles of the dynamic second hyperpolarizability are identical to the poles of the dynamic polarizability (82), i.e., the one-electron excitations of adiabatic LR-TD-DFT. Interestingly, two-electron excitations are accessible via sequential absorption in real-time TDHF and TD-DFT (83).

The second problem associated with f_{xc} (also found in v_{xc} and E_{xc}) is the "scale-up catastrophe," so called because it arises when a system is made increasingly larger. Within DFT, an important goal is to extrapolate ab initio accuracy to molecules too large to otherwise treat by conventional (i.e., HF-based) ab initio wave-function calculations. The usual recommendation is to test DFT calculations on small molecules where comparisons can be made with accurate ab initio calculations and then to assume that DFT calculations that are reliable for a given class of molecule and molecular properties will remain accurate as the size of the molecules treated is increased (i.e., scaled-up). When inaccuracies increase as the size of the system is increased, then we have a scale-up catastrophe. An example of a scale-up catastrophe in LR-TD-DFT occurs in periodic systems where the xc-kernel vanishes on the lower rungs of our Jacob's ladder as a result of improper scaling with respect to the number of K points (84). When this occurs, the first vertical excitation energy reduces to the difference between the HOMO and LUMO orbital energies, which is too low. Nevertheless, the spectrum may remain essentially correct because the oscillator strength of this transition may be negligible.

Studies on oligomers of conducting polymers provide a well-known and disturbing example of a scale-up catastrophe: Dynamic polarizabilities can be overestimated by arbitrarily large amounts by simply going to a large enough oligomer (85–86). There are different ways to try to understand this error. For example, most DFAs are based on the homogeneous electron gas, which is a model for a perfect conductor. Applying an electric field to a conductor leads to the buildup of surface charges that cancel the applied fields in the interior of the conductor (i.e., the Faraday effect). If the system behaves too much like a conductor, then the HOMO-LUMO gap is too small owing to, for example, an improper description of the PNDD. Although this explanation mainly uses orbital energy terms and v_{xc}, the reaction field that cancels the applied field in the interior of the conductor is given by the response of the SCF, which depends on the description of the xc-kernel. This xc-kernel must be "ultranonlocal" in the sense that it must react to charges built up on the surface of the conductor. On the lower rungs of Jacob's ladder, $f_{xc}^{\sigma_1,\sigma_2}(\mathbf{r}_1, \mathbf{r}_2)$ is roughly diagonal in $(\mathbf{r}_1, \mathbf{r}_2)$. This is in contradiction with a rough estimate, exact in the case of two-electron systems, of the exchange-only part of the xc-kernel, which suggests that it be more like $-|\gamma(\mathbf{r}_1, \mathbf{r}_2)|^2/(\rho(\mathbf{r}_1)\mathbf{r}_{12}\rho(\mathbf{r}_2))$ (87). Thus, we conclude that a diagonal f_{xc} is incorrect. Few choices are available to deal with this problem: either we restrict our studies to medium-sized systems and avoid the onset of the scale-up catastrophe, or we climb Jacob's ladder to use more sophisticated functionals. One way to restrict studies to medium-sized systems is to use a subsystem theory such as is employed to treat excitons in light-harvesting complex II, so that TD-DFT is restricted to only medium-sized molecules at any given moment. Climbing Jacob's ladder, we can use range-separated hybrids as well as functionals with contributions from the HF exchange (88–91). Using TD current-density functional with the Vignale-Kohn functional (45, 92) is also helpful because the current can carry information about perturbations at a distance.

5. GOING BEYOND THE ADIABATIC APPROXIMATION

The exact TD-DFT potential (Equation 33) is a functional of the whole history of past densities and the initial conditions. These memory effects are completely neglected in common TD-DFT applications using the AA. In fact, the AA assumes that the xc-potential reacts instantaneously and without memory and so may be expressed in terms of the ordinary DFT xc-energy evaluated for the density at that time,

$$v_{xc}^{\sigma}(\mathbf{r}, t) = \frac{\delta E_{xc}[\rho_\alpha^t, \rho_\beta^t]}{\delta \rho_\sigma^t(\mathbf{r})}. \tag{39}$$

Thus, the AA xc-potential is only a functional of the function $\rho_\sigma^t(\mathbf{r})$ of the three independent variables $\mathbf{r} = (x, y, z)$ at a fixed time and not a functional of the full function $\rho_\sigma(\mathbf{r}, t)$ of four independent variables, a fact that we have tried to emphasize by our choice of notation. In this sense, TD-DFAs using the AA work fairly well when the noninteracting system is a reasonable physical first approximation to the interacting system, but they fail dramatically in cases such as 2p2h excited states (93), conical intersections (18, 68), charge transfers and Rydberg excitations (74, 78), excited states along the bond dissociation coordinate (94), one-dimensional extended systems (95, 96), band-gaps in solids (97), and spectra of semiconductors (97–99). In such cases, the contribution of past densities to the xc-energy becomes essential, requiring memory functionals specifically designed for TD-DFT. In this section, we review the most successful memory functionals currently available. Few attempts have been made to approximate the xc-action directly (100). Instead, most memory functionals approximate the derivatives. Therefore, our discussion focuses on the construction of memory xc-potentials, memory xc-kernels.

Memory introduces strong requirements for TD-DFT functionals (101), which forbid the intuitively simple functional approximations of ground-state DFT. For example, a simple parameterization of a spatially local memory LDA xc-kernel for the homogeneous electron gas (102) violates, by construction, the zero-force theorem (31, 103), introducing unphysical damping effects during the time propagation of the density and a corresponding loss of total energy. Several schemes have appeared enforcing the sum rules a posteriori (104, 105). Most importantly, these studies showed that memory functionals must be nonlocal in space. This property forbids the application of the popular gradient expansion to memory functionals (106), ultimately a consequence of the ultranonlocality property of the exact xc-functional.

5.1. Current and Lagrangian Density-Functional Theory

The ultranonlocality property of the exact functional indicates that the density may not be the best reduced variable to express TD xc-effects. This redirected the attention to other TD theories where memory effects are described by local functionals, such as in TD-CDFT (100, 106–109) and Lagrangian TD-DFT (110–112).

TD-CDFT is very related to TD-DFT, though its range of applications is broader. In fact, the one-to-one correspondence between currents and external potentials is the first step in the Runge-Gross existence proof for TD-DFT (3). However, the TD-CDFT proof does not resort to any surface integral, which makes its application to solids more straightforward than that of TD-DFT. Vignale and Kohn provided the first memory functional for TD-CDFT, which consists of a parameterization of a memory LDA xc-kernel tensor for the homogeneous electron gas (106). This kernel is local in space, and unlike the corresponding kernel in TD-DFT, it satisfies the zero-force theorem. However, the kernel introduces damping effects that are too strong to induce a decoherence mechanism, which allows the density to decay back to a ground state with higher entropy, different from the real ground state in which the total energy is conserved (113). The Vignale-Kohn kernel has been used successfully to calculate the static polarizabilities of one-dimensional conjugated chains, which were largely overestimated by common adiabatic LDA (95). However, it fails for one-dimensional hydrogen chains, requiring more sophisticated kernels (96). The Vignale-Kohn kernel also shows the characteristic double-peak spectrum of bulk silicon (114), a feature that is not present in the adiabatic LDA spectrum. Memory kernels of TD-CDFT can then be mapped onto TD-DFT kernels while maintaining part of the features of the Vignale-Kohn kernel (115).

Lagrangian TD-DFT has fewer applications to realistic systems, but it has provided deeper insight on the role of memory. Lagrangian TD-DFT is a reformulation of TD-DFT, in which the electronic density is re-expressed in a reference (Lagrangian) frame that moves along with the fluid (110, 111). This allows the memory to be expressed locally in terms of a the position of fluid elements and the deformation tensor. The deformation tensor accounts for the Coulomb coupling of a differential volume of fluid at position $\mathbf{r}$ and time t, which was at a different position $\mathbf{r}'$ at an earlier time $t' < t$. Both TD-CDFT and Lagrangian TD-DFT are equivalent in the linear regime (112).

5.2. Optimized Effective Potential Approaches

All the aforementioned memory functionals lack a systematic route to improve the present approximations. A more systematic way to construct memory functionals is to use the TD-OEP, in which many-body perturbation theory (MBPT) quantities are mapped onto TD-DFT (116–122). An easy way to establish this mapping is to use the Kohn-Sham assumption, which requires

that the interacting TD density equal the noninteracting one (118). This is the basis of the TD Sham-Schlüter equation, which allows us to relate the self-energy to the xc-potential and the kernel of the Bethe-Salpeter equation to the xc-kernel. In this way, consistent approximations that guarantee the satisfaction of exact conditions are possible (120). There are many ways to derive the TD Sham-Schlüter equation, but similar functionals are obtained if the same MBPT approximation is used. A simple way to derive xc-kernels requires that the diagonal of the MBPT response functions lead to the same spectrum as the TD-DFT response function (Equation 22), which leads to

MBPT: many-body perturbation theory

$$f_{xc}(\mathbf{r},\mathbf{r}';\omega) = \int d^3r_1 \int d^3r_2 \int d^3r_3 \int d^3r_4 \Lambda(\mathbf{r};\mathbf{r}_1,\mathbf{r}_2;\omega) K(\mathbf{r}_1,\mathbf{r}_2;\mathbf{r}_3,\mathbf{r}_4;\omega) \Lambda_s^{\dagger}(\mathbf{r}_3,\mathbf{r}_4;\mathbf{r}';\omega), \quad (40)$$

relating the exact TD-DFT xc-kernel to the kernel $K(\omega) = \Pi_s^{-1}(\omega) - \Pi^{-1}(\omega)$ defined from the polarization propagator from MBPT (122). The mapping is possible thanks to the localization function Λ, which is expressed in terms of the response functions (Equation 22):

$$\Lambda(\mathbf{r}_1;\mathbf{r}_2,\mathbf{r}_3;\omega) = \chi^{-1}(\mathbf{r}_1,\mathbf{r}_2;\omega)\chi(\mathbf{r}_2,\mathbf{r}_3;\omega). \quad (41)$$

The localizer Λ_s, appearing in Equation 40, is defined as in Equation 41 except in terms of the noninteracting response function ($\chi_s(\omega)$). The localizer introduces an extra frequency dependence in the kernel, which brings the ultranonlocality property of the exact TD-DFT functional into the MBPT quantity (121–124). To date, little is known about the exact role of the localization step, despite its interesting properties. For example, Gonze & Scheffler (123) showed that, when one applies the linear Sham-Schlüter equation in Equation 41, the single-pole approximation gives

$$\omega_{ia} = \Delta\varepsilon_{ia} + (ia|f_{xc}(\Delta\varepsilon_{ia})|ai) = \Delta\varepsilon_{ia} + (ii|K(\Delta\varepsilon_{ia})|aa), \quad (42)$$

where $\Delta\varepsilon_{ia} = \varepsilon_a - \varepsilon_i$. In fact, a cancellation of the localizer is observed, and the exact xc-kernel is equal to a different matrix element of the kernel derived from the MBPT quantities. A general treatment of localization is plagued with numerical problems, owing to the difficulties in inverting the singular density response functions that are involved (125, 126). In the linear-response regime, an interesting work-around can be used to account fully for the localization effects without the need of explicitly inverting any response function. This is achieved by re-expressing LR-TD-DFT as the response of the noninteracting potential (127).

Using a first-order approximation of K, one obtains the TD-EXX kernel (117, 119, 120, 122). Given the correct asymptotic decay of exchange, this kernel provides the correct description of charge transfer (78) and the correct position of the continuum states (6). Although the exchange kernel in MBPT is frequency independent, the full TD-EXX is a frequency-dependent functional (117, 126) as a result of the localizer Λ. Therefore, some (minor) memory effects are taken into account (128). In general, the frequency dependence of the localizer in the TD-EXX is not enough to include excitations with two or more particle-hole pairs (129, 130), and frequency-dependent MBPT kernels are required (80, 122, 131, 132).

The lack of 2p2h excitations is an endemic problem of the AA (6). These poles should be present, because TD-DFT is formally exact. However, they are not present when an adiabatic xc-kernel is used in the LR-TD-DFT equations. Because the number of solutions of Equation 36 is given by the dimension of the matrices, that is, the number of 1p1h states, recovering 2p2h states requires frequency-dependent xc-kernels (93, 133), which make the LR-TD-DFT equations nonlinear and extra solutions appear. Frequency dependence can be included via the solution of a Sham-Schlüter equation. The MBPT kernel of the Bethe-Salpeter equation has to be constructed carefully; otherwise, the resulting xc-kernel may introduce spurious transitions (131, 132).

CV: constrained variational

The first successful ω-dependent xc-kernel came from the dressed TD-DFT first proposed by Burke and coworkers (93, 133) to include one 2p2h at a time and later generalized to any number of 2p2h states by using full-featured MBPT techniques (80, 122). The kernel of dressed TD-DFT can be viewed as a hybrid kernel between the adiabatic xc-kernel and the frequency-dependent part of the MBPT kernel,

$$f_{xc}(\mathbf{r}, \mathbf{r}'; \omega) = f_{xc}^{AA}(\mathbf{r}, \mathbf{r}') + K^{\omega}(\mathbf{r}, \mathbf{r}; \mathbf{r}', \mathbf{r}'; \omega), \quad (43)$$

where $K^{\omega}(\mathbf{r}, \mathbf{r}; \mathbf{r}', \mathbf{r}'; \omega)$ corresponds to the frequency-dependent part of the kernel derived from a second-order polarization propagator approach (for the mathematical expression, see References 122 and 6). Several variations (see Reference 134) on dressed TD-DFT are possible. In addition, comparison of the performance of dressed TD-DFT against benchmark ab initio results for 28 organic chromophores has gone far toward establishing the best protocols.

5.3. Time-Dependent Reduced Density-Matrix Functional Theory

Giesbertz and coworkers have conducted important recent work extending RDMFT to the TD case (94, 135–140). However, most of these attempts fail to obtain the correct $\omega \to 0$ limit of the AA for TD-RDMFT even for two-electron systems (139). If the orbitals and occupation numbers in the TD response equations as well as their phases are included, then exact solutions are obtained for two-electron systems (138). The importance of phases in this case is reminiscent of our observations regarding spin-wave instabilities and violation of NVR, providing further proof of the need to include phase information in TD-DFT. Note that this phase information is not included in the 1-RDM. Thus, we need a new functional dependence that goes beyond the density matrix, perhaps one that is assimilated with a memory effect.

6. GOING AROUND THE ADIABATIC APPROXIMATION

In the previous section, we described progress in TD-DFT going beyond the AA but trying to keep the essential spirit of TD-DFT. In this section, we describe approaches that try to solve the problems of the TD-DFT AA while retaining something resembling the frequency-independent kernel. These may be thought of as ways to go around the problem.

6.1. Reconciling TD-DFT and ΔSCF

As described above, the ΔSCF method and its MSM variant predate TD-DFT in quantum chemistry. The older method is particularly well justified for calculating the first ionization potentials and electron affinities, the lowest triplet excitation, and, perhaps, transitions in general to states dominated by a single configuration. Indeed, the numbers produced by the MSM ΔSCF method and TD-DFT are often quite similar, though the formulae are different, thereby presenting a puzzle since the beginning of applications of TD-DFT in quantum chemistry (4). Reconciling the two methods may also allow some of the better aspects of the MSM ΔSCF method to be used in TD-DFT, namely the ease of handling 2p2h and higher-ph excitations in the ΔSCF method or the ability to describe density relaxation better during excitation. A first step in this direction were presented by one of us in 1999 (see Reference 141). These ideas were later used to develop a charge-transfer correction for TD-DFT (13). Hu et al. followed up this work to develop their own approach to correcting problems with underestimated Rydberg and charge-transfer excitations (142, 143).

Ziegler's group in Alberta recently followed up on these ideas using the form of constrained variational DFT (CV-DFT) (144–147). The energy is to be minimized with respect to the

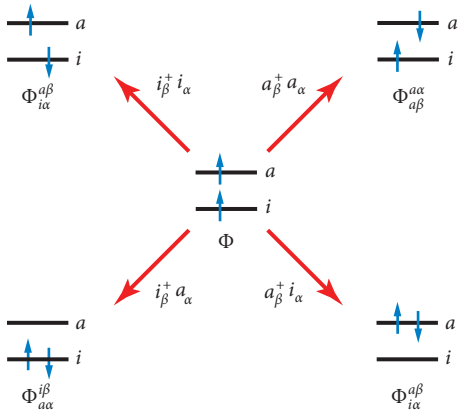

Figure 4

Schematic of spin-flip excitations in the two-orbital two-electron model.

transformation, $\phi_i' = \phi_i + \sum_a U_{a,i}\phi_a + \mathcal{O}^{(2)}(U)$, of the Kohn-Sham orbitals, subject to the constraint $\vec{U}^\dagger\vec{U} = 1$. The second-order CV(2)-DFT energy expression is already familiar from stability analysis (Equation 21 with $\lambda = 1$). Minimizing to this order gives only the TD-DFT TDA. However, fourth-order CV(4)-DFT with relaxed orbitals gives a much improved treatment of charge-transfer excitations without including any nonadiabatic frequency dependence (148).

6.2. Spin-Flip TD-DFT

Another way to go around the AA—this time to access a 2p2h excitation—is to use the spin-flip method. The basic idea is illustrated in the TOTEM in **Figure 4**. To do this properly, we must consider the Kohn-Sham orbitals as spinors, $(\psi_\alpha(\mathbf{r}), \psi_\beta(\mathbf{r}))$, which can rotate their spin direction at different points in physical space. The density also acquires spin labels,

$$\rho(\mathbf{r}) = \begin{bmatrix} \rho_{\alpha,\alpha}(\mathbf{r}) & \rho_{\alpha,\beta}(\mathbf{r}) \\ \rho_{\beta,\alpha}(\mathbf{r}) & \rho_{\alpha,\alpha}(\mathbf{r}) \end{bmatrix}. \tag{44}$$

Thus, the xc-kernel, $f_{xc}^{\sigma_1,\sigma_2;\tau_1,\tau_2}(\mathbf{r},\mathbf{r}')$, also acquires additional labels but for the sole purpose of deriving a more general LR-TD-DFT equation. Ultimately, we will evaluate the xc-kernel using the usual collinear Kohn-Sham theory (i.e., each spin orbital is either α or β but not some linear combination of the two). However, conventional pure DFAs do not allow spin flips.

To obtain good agreement with experiment, Krylov and coworkers (149, 150) used a significantly higher amount of HF exchange (50%) than is typically used for ground-state properties (~25%). Even higher percentages of HF exchange (>50%) are necessary for calculating second hyperpolarizabilities of diradical systems by this spin-flip method (151). Although the use of a different functional for ground and excited states is disturbing, the basic idea is admirable and this method continues to be used (151–153). In particular, this is the spin-flip TD-DFT approach mentioned in Section 1 in the context of its recent use by Minezawa & Gordon (154), who found the method gave a relatively good description of conical intersections in ethylene.

The next and most recent major advance in spin-flip TD-DFT came with an article by Wang & Ziegler (155), which is intimately related to work by Liu and coworkers on relativistic four-component TD-DFT (156). Wang & Ziegler (155) proposed that any pure spin-density

xc-functional, $E_{xc}[\rho_\alpha, \rho_\beta]$, could be used to make a noncollinear xc-functional suitable for spin-flip calculations by making the substitutions

$$\rho_\alpha \to \rho_+ = \frac{1}{2}(\rho + s) \text{ and } \rho_\beta \to \rho_- = \frac{1}{2}(\rho - s) \tag{45}$$

involving two quantities that are invariant under a unitary transformation of the spin coordinates. These quantities are the total charge density, $\rho = \rho_{\alpha,\alpha} + \rho_{\beta,\beta}$, and the magnetization, s, whose square is given by $s^2 = (\rho_{\alpha,\alpha} - \rho_{\beta,\beta})^2 + 2(\rho_{\alpha,\beta}^2 + \rho_{\beta,\alpha}^2)$. The collinear limit of s is the spin polarization $s \to \rho_\alpha - \rho_\beta$ after an appropriate choice of phase. The factor of 1/2 has been introduced by us (63) so that

$$\rho_+ \to \rho_\alpha, \quad \rho_- \to \rho_\beta \tag{46}$$

in the same limit. After taking derivatives and the noncollinear limit, the xc-kernel becomes

$$\begin{bmatrix} f_{xc}^{\alpha,\alpha;\alpha,\alpha} & f_{xc}^{\alpha,\alpha;\beta,\beta} & f_{xc}^{\alpha,\alpha;\alpha,\beta} & f_{xc}^{\alpha,\alpha;\beta,\alpha} \\ f_{xc}^{\beta,\beta;\alpha,\alpha} & f_{xc}^{\beta,\beta;\beta,\beta} & f_{xc}^{\beta,\beta;\alpha,\beta} & f_{xc}^{\beta,\beta;\beta,\alpha} \\ f_{xc}^{\alpha,\beta;\alpha,\alpha} & f_{xc}^{\alpha,\beta;\beta,\beta} & f_{xc}^{\alpha,\beta;\alpha,\beta} & f_{xc}^{\alpha,\beta;\beta,\alpha} \\ f_{xc}^{\beta,\alpha;\alpha,\alpha} & f_{xc}^{\beta,\alpha;\beta\beta} & f_{xc}^{\beta,\alpha;\alpha,\beta} & f_{xc}^{\beta,\alpha;\beta,\alpha} \end{bmatrix} = \begin{bmatrix} f_{xc}^{\alpha,\alpha} & f_{xc}^{\alpha,\beta} & 0 & 0 \\ f_{xc}^{\beta,\alpha} & f_{xc}^{\beta,\beta} & 0 & 0 \\ 0 & 0 & \frac{v_{xc}^{\alpha} - v_{xc}^{\beta}}{\rho_\alpha - \rho_\beta} & 0 \\ 0 & 0 & 0 & \frac{v_{xc}^{\alpha} - v_{xc}^{\beta}}{\rho_\alpha - \rho_\beta} \end{bmatrix}. \tag{47}$$

This approach to spin-flip TD-DFT has been applied to the dissociation of H_2 (155) and to calculate the spectra of open-shell molecules (157–159). We have applied the Wang-Ziegler approach to the photochemical ring opening of oxirane (H_2COCH_2) (63). Although this approach definitely overcame the cusp problem for the C_{2v} ring opening and does allow coupling of the ground and excited states so that there is a true conical intersection, the position of the conical intersection is intermediate between the CIS seam and the complete active-space SCF conical intersection (63). Very recently, analytical derivatives have been worked out for the Wang-Ziegler method (160).

The Wang-Ziegler approach has also been proposed (161) and applied (162) as the basis of a more general spin-coupled TD-DFT. Very recently, it has been used to solve the problem of spin adaption for LR-TD-DFT in open-shell molecules (163, 164) that had been highlighted by earlier work on spin contamination in TD-DFT (165). Hybrid spin-flip functionals are also beginning to appear (162, 166).

7. PERSPECTIVES

In coming to the final section of this review, we are deeply conscious of the many aspects of TD-DFT that we have neglected and the shallowness of our treatment of those aspects of TD-DFT that we have been able to treat in this overview of what has become a vast field. Nevertheless, we hope that the reader has appreciated the historical interplay between DFT, TD-DFT, and the development of DFAs. In seeking to calculate new types of properties, TD-DFT has brought into sharper focus known problems of and has placed new demands on DFAs. This, in turn, has propelled further improvement of DFAs for classical DFT as well as a more detailed exploration of Jacob's ladder.

Also significant has been the difficulty of answering the Runge-Gross challenge to go beyond the AA and include memory in TD-DFT. Section 5 discusses methods for trying to go beyond the AA while preserving the true spirit of (TD-)DFT—that is, to do as much work analytically before asking the computer to do the work. In the end, this means taking things from MBPT and putting them into the functionals. Doing the opposite—that is, adding MBPT on top of the functionals—is an indication that there is something we do not yet understand well enough and need to explore further.

The penultimate section (Section 6) discusses primarily pragmatic ways to try to circumvent problems created by the AA without abandoning the AA. These, plus dressed TD-DFT (Section 5), are the tools we have now but that may merge in the future with the more rigorous approaches of Section 5 to give something approaching an answer to the Runge-Gross challenge.

Only time will tell . . . but then time is such an important and fundamental physical parameter!

SUMMARY POINTS

1. After almost three decades, the Runge-Gross theorem is largely uncontested as the foundations of a rigorous theory. Initial problems in the definition of the action have been heavily investigated, leading to increasingly satisfactory definitions of appropriate xc-actions. Now, most fundamental TD-DFT research is devoted to improving TD-DFAs.
2. TD-DFT is making good progress toward a general application to photochemical problems. Charge transfer, Rydberg excited states, and 2p/2h states can now be correctly treated within LR-TD-DFT. The treatment of conical intersections will require overcoming the NVR problem in DFT, which requires fractional occupation numbers and possibly complex orbitals.
3. In general, LR-TD-DFT using the Tamm-Dancoff approximation leads to better excitation energies and should be preferred when calculating PESs. However, the Tamm-Dancoff approximation can lead to inaccurate oscillator strength distributions.
4. Most of the problems attributed to LR-TD-DFT can be resolved by using decent approximations of the DFT functionals. From practical experience, asymptotically corrected hybrid functionals with 20–25% of HF exchange lead to the best results for singly excited states of finite systems.
5. Memory functionals have extended the range of applicability of TD-DFT, though some problems remain unresolved. The long-standing problem of 2p/2h states can be resolved by adding to the AA a frequency-dependent component derived with the help of MBPT techniques. Though the mixture requires careful application to avoid double counting of correlation, present applications show encouraging results.
6. Spin-flip LR-TD-DFT currently offers a practical solution for photochemical problems. It adds some double-excitation character and avoids regions of the PES with NVR problems, offering an easy route to calculate conical intersections. Also, it can successfully treat excited states of some open-shell systems.

FUTURE ISSUES

1. Even though some advances have been made, memory functionals are still in their infancy, and better functionals are necessary to extend the range of application of TD-DFT. It seems more appropriate to think in terms of a different Jacob's ladder for memory functionals in TD-DFT with the rungs defined according to the functional dependence as follows: TD-DFT (density), TD-CDFT (density and current), L-TDDFT (fluid position and deformation tensor), TD-OEP (orbitals), and TD-RDMFT (1-electron density matrix, orbital phase).

2. A general application of TD-DFT to photochemistry will require more sophisticated functionals, probably depending on additional parameters other than just the density. Studies of TD-RDMFT indicate that TD-DFT functionals may also need as variables the occupation number and the TD phase of the orbitals.

DISCLOSURE STATEMENT

The authors are not aware of any affiliations, memberships, funding, or financial holding that might be perceived as affecting the objectivity of this review.

ACKNOWLEDGMENTS

M. H.-R. acknowledges a scholarship from the French Ministry of Education. This work has been carried out in the context of the French Rhône-Alpes *Réseau thématique de recherche avancée (RTRA): Nanosciences aux limites de la nanoélectronique* and the Rhône-Alpes Associated Node of the European Theoretical Spectroscopy Facility (ETSF). We thank Klaas Giesbertz for sending us a copy of his doctoral thesis. Evert Jan Baerends, Christoph Jacob, Melvin Levy, Johannes Neugebauer, Lucia Reining, Gustavo Scuseria, and Tomasz Wesołowski are thanked for their helpful conversations.

LITERATURE CITED

1. Hohenberg P, Kohn W. 1964. Inhomogenous electron gas. *Phys. Rev.* 136:B864
2. Kohn W, Sham LJ. 1965. Self-consistent equations including exchange and correlation effects. *Phys. Rev.* 140:A1133
3. Runge E, Gross EKU. 1984. Density-functional theory for time-dependent systems. *Phys. Rev. Lett.* 52:997
4. Casida ME. 1995. Time-dependent density-functional response theory for molecules. In *Recent Advances in Density Functional Methods, Part I*, ed. DP Chong, p. 155. Singapore: World Sci.
5. Casida ME. 2009. Review: time-dependent density-functional theory for molecules and molecular solids. *J. Mol. Struct.* 914:3
6. Baer R, Kronik L, Kummel S, eds. 2011. Special volume: Open problems and new solutions in time dependent density functional theory. *Chem. Phys.* 391
7. Marques MAL, Maitra N, Nogueira F, Gross EKU, Rubio A, eds. 2012. *Fundamentals of Time-Dependent Density Functional Theory*. Lect. Notes Phys. Vol. 837. New York: Springer-Verlag
8. Marques MAL, Gross EKU. 2004. Time-dependent density-functional theory. *Annu. Rev. Phys. Chem.* 55:427
9. Koopmans T. 1934. Über die Zuordnung von Wellenfunktionen und Eigenwerten zu den Einzelnen Elektronen Eines Atoms. *Physica* 1:104
10. Jørgensen P, Simons J. 1981. *Second Quantization-Based Methods in Quantum Chemistry*. New York: Academic
11. Ortiz JV. 1994. One-electron density-matrices and energy gradients in the random-phase approximation. *J. Chem. Phys.* 101:6743
12. Ziegler T, Rauk A, Baerends J. 1977. Calculation of multiplet energies by Hartree-Fock-Slater method. *Theor. Chim. Acta* 43:261
13. Casida ME, Gutierrez F, Guan J, Gadea FX, Salahub DR, Daudey JP. 2000. Charge-transfer correction for improved time-dependent local density approximation excited-state potential energy curves: analysis within the two-level model with illustration for H_2 and LiH. *J. Chem. Phys.* 113:7062

14. Casida ME. 2008. TDDFT for excited states. In *Computational Methods in Catalysis and Materials Science*, ed. P Sautet, RA van Santen, p. 33. Weinheim, Ger.: Wiley-VCH
15. Ågren H, Carravetta V, Vahtras O, Pettersson LGM. 1997. Direct SCF direct static exchange calcuations of electronic spectra. *Theor. Chem. Acc.* 97:14
16. Fukutome H. 1981. Unrestricted Hartree-Fock theory and its applications to molecules and chemical reactions. *Int. J. Quantum Chem.* 20:955
17. Dreizler RM, Gross EKU. 1990. *Density Functional Theory: An Approach to the Quantum Many-Body Problem*. New York: Springer-Verlag
18. Cordova F, Jourbet Doriol L, Ipatov A, Casida ME, Filippi C, Vela A. 2007. Troubleshooting time-dependent density-functional theory for photochemical applications: oxirane. *J. Chem. Phys.* 127:164111
19. Tapavicza E, Tavernelli I, Rothlisberger U, Filippi C, Casida ME. 2008. Mixed time-dependent density-functional theory/classical surface hopping study of oxirane photochemistry. *J. Chem. Phys.* 129:124108
20. Ostland NS. 1972. Complex and unrestricted Hartree-Fock wave functions. *J. Chem. Phys.* 57:2994
21. Schiper PRT, Gritsenko OV, Baerends EJ. 1999. Benchmark calculations in density functional theory: comparison of the accurate Kohn-Sham solution with generalized gradient approximations for the $H_2 + H$ and $H_2 + H_2$ reactions. *J. Chem. Phys.* 111:4056
22. Casida ME. 2002. Jacob's ladder for time-dependent density-functional theory: some rungs on the way to photochemical heaven. In *Accurate Description of Low-Lying Molecular States and Potential Energy Surfaces*, ed. MRH Hoffmann, KG Dyall, p. 199. Washington, DC: ACS
23. Perdew JP, Schmidt K. 2001. Jacob's ladder of density functional approximations for the exchange-correlation energy. In *Density Functional Theory and Its Applications to Materials*, ed. VE Van Doren, K Van Alseoy, P Geerlings, p. 1. Melville, NY: Am. Inst. Phys.
24. Head-Gordon M, Artacho E. 2008. Chemistry on the computer. *Phys. Today* 61(4):58
25. Wesołowski TA, Warshel A. 1993. Frozen density functional approach for ab initio calculations of solvated molecules. *J. Phys. Chem.* 97:8050
26. Wesołowski T. 2008. Embedding a multideterminantal wave function in an orbital-free environment. *Phys. Rev. A* 77:012504
27. Casida ME, Wesołowski TA. 2004. Generalization of the Kohn-Sham equations with constrained electron density (KSCED) formalism and its time-dependent response theory formulation. *Int. J. Quantum Chem.* 96:577
28. Jacob CR, Visscher L. 2008. A subsystem density-functional theory approach for the quantum chemical treatment of proteins. *J. Chem. Phys.* 128:155102
29. Frauenheim T, Seifert G, Elsterner M, Hajnal Z, Jungnickel G, et al. 2000. A self-consistent charge density-functional based tight-binding method for predictive materials simulations in physics, chemistry and biology. *Phys. Stat. Sol. B* 217:41
30. Singh R, Deb BM. 1999. Developments in excited-state density-functional theory. *Phys. Rep.* 311:50
30a. Daul C. 1994. Density functional theory applied to the excited states of coordination compounds. *Int. J. Quantum Chem.* 52:867
31. Dobson JF. 1994. Harmonic-potential theorem: implications for approximate many-body theories. *Phys. Rev. Lett.* 73:2244
32. Dirac PAM. 1930. Note on exchange phenomena in the Thomas atom. *Proc. Camb. Philos. Soc.* 26:376
33. Frenkel J. 1934. *Wave Mechanics, Advanced General Theory*. Oxford: Clarendon
34. Langhoff PW, Epstein ST, Karplus M. 1972. Aspects of time-dependent perturbation theory. *Rev. Mod. Phys.* 44:602
35. Vignale G. 2008. Real-time resolution of the causality paradox of time-dependent density-functional theory. *Phys. Rev. A* 77:062511
36. Zangwill A, Soven P. 1980. Density-functional approach to local-field effects in finite systems: photoabsorption in the rare gases. *Phys. Rev. A* 21:1561
37. Xu BX, Dhara AK. 1985. Current density-functional theory for time-dependent systems. *Phys. Rev. A* 31:2682
38. Dhara AK, Ghosh SK. 1987. Density-functional theory for time-dependent systems. *Phys. Rev. A* 35:442
39. Gross EKU, Kohn W. 1990. Time-dependent density-functional theory. *Adv. Quantum Chem.* 21:255

40. Rajagopal AK. 1996. Time-dependent variational principle and the effective action in density-functional theory and Berrys phase. *Phys. Rev. A* 54:3916
41. van Leeuwen R. 1998. Causality and symmetry in time-dependent density-functional theory. *Phys. Rev. Lett.* 80:1280
42. van Leeuwen R. 2001. Key concepts in time-dependent density-functional theory. *Int. J. Mod. Phys. B* 15:1969
43. Mukamel S. 2005. Generalized time-dependent density-functional-theory response functions for spontaneous density fluctuations and nonlinear response: resolving the causality paradox in real time. *Phys. Rev. A* 71:024503
44. Ghosh SK, Dhara AK. 1988. Density-functional theory of many-electron systems subjected to time-dependent electric and magnetic fields. *Phys. Rev. A* 38:1149
45. Faassen MV. 2006. Time-dependent current-density-functional theory applied to atoms and molecules. *Int. J. Mod. Phys. B* 20:3419
46. Saue T, Jensen HJA. 2003. Linear response at the 4-component relativistic level: application to the frequency-dependent dipole polarizabilities of the coinage metal dimers. *J. Chem. Phys.* 118:522
47. Castro A, Marques MAL, Appel H, Oliveira M, Rozzi CA, et al. 2006. Octopus: a tool for the application of time-dependent density functional theory. *Phys. Status Solidi* 243:2465
48. Hirata S, Head-Gordon M. 1999. Time-dependent density functional theory within the Tamm-Dancoff approximation. *Chem. Phys. Lett.* 314:291
49. Jamorski C, Casida ME, Salahub DR. 1996. Dynamic polarizabilities and excitation spectra from a molecular implementation of time-dependent density-functional response theory: N_2 as a case study. *J. Chem. Phys.* 104:5134
50. Grüning M, Marini A, Gonze X. 2009. Exciton-plasmon states in nanoscale materials: breakdown of the Tamm-Dancoff approximation. *Nano Lett.* 9:2820
51. Casida ME, Natarajan B, Deutsch T. 2012. Non-Born–Oppenheimer dynamics and conical intersections. See Ref. 7, p. 279
52. Tapavicza E, Tavernelli I, Rothlisberger U. 2007. Trajectory surface hopping within linear response time-dependent density-functional theory. *Phys. Rev. Lett.* 98:023001
53. Barbatti M, Pitner J, Pederzoli M, Werner U, Mitrić R, et al. 2010. Non-adiabatic dynamics of pyrrole: dependence of deactivation mechanisms on the excitation energy. *Chem. Phys.* 375:26
54. Send R, Furche F. 2010. First-order nonadiabatic couplings from time-dependent hybrid density-functional response theory: consistent formalism, implementation, and performance. *J. Chem. Phys.* 132:044107
55. Duncan WR, Prezhdo OV. 2007. Theoretical studies of photoinduced electron transfer in dye-sensitized TiO_2. *Annu. Rev. Phys. Chem.* 58:143
56. Rocca D, Gebauer R, Angelis FD, Nazeeruddin MK, Baroni S. 2009. Time-dependent density functional study of squaraine dye-sensitized solar cells. *Chem. Phys. Lett.* 475:49
57. Neugebauer J. 2007. Couplings between electronic transitions in a subsystem formulation of time-dependent density functional theory. *J. Chem. Phys.* 126:134116
58. Neugebauer J. 2008. Photophysical properties of natural light-harvesting complexes studied by subsystem density-functional theory. *J. Phys. Chem. B* 112:2207
59. König C, Neugebauer J. 2011. First-principles calculation of light-harvesting complex II. *Phys. Chem. Chem. Phys.* 13:10475
60. Niehaus TA. 2009. Approximate time-dependent density functional theory. *J. Mol. Struct.* 914:38
61. Bauernschmitt R, Ahlrichs R. 1996. Stability analysis for solutions of the closed-shell Kohn-Sham equation. *J. Chem. Phys.* 104:9047
62. Casida ME, Ipatov A, Cordova F. 2006. Linear-response time-dependent density-functional theory for open-shell molecules. See Ref. 167, p. 243
63. Huix-Rotllant M, Natarajan B, Ipatov A, Wawire CM, Deutsch T, Casida ME. 2010. Assessment of noncollinear spin-flip Tamm-Dancoff approximation time-dependent density-functional theory for the photochemical ring-opening of oxirane. *Phys. Chem. Chem. Phys.* 12:12811
64. Löwdin PO, Shull H. 1956. Natural orbitals in the quantum theory of two-electron systems. *Phys. Rev.* 101:1730

65. Müller AMK. 1984. Explicit approximate relation between reduced two- and one-particle density matrices. *Phys. Lett. A* 105:446
66. Goedecker S, Umrigar C. 1998. Natural orbital functional for the many-electron problem. *Phys. Rev. Lett.* 81:866
67. Lathiotakis NN, Sharma S, Dewhurst JK, Eich FG, Marques MAL, Gross EKU. 2009. Density-matrix-power functional: performance for finite systems and the homogeneous electron gas. *Phys. Rev. A* 79:040501
68. Levine BG, Ko C, Quenneville J, Martinez TJ. 2006. Conical intersections and double excitations in density functional theory. *Mol. Phys.* 104:1039
69. Casida ME, Jamorski C, Casida KC, Salahub DR. 1998. Molecular excitation energies to high-lying bound states from time-dependent density-functional response theory: characterization and correction of the time-dependent local density approximation ionization threshold. *J. Chem. Phys.* 108:4439
70. Wasserman A, Maitra NT, Burke K. 2003. Accurate Rydberg excitations from the local-density approximation. *Phys. Rev. Lett.* 91:263001
71. Hirata S, Zhan CG, Apra E, Windlus TL, Dixon DA. 2003. A new, self-contained asymptotic correction scheme to exchange-correlation potentials for time-dependent density functional theory. *J. Phys. Chem. A* 107:10154
72. Casida ME, Casida KC, Salahub DR. 1998. Excited-state potential energy curves from time-dependent density-functional theory: a cross section of formaldehyde's $^1A_1$ manifold. *Int. J. Quantum Chem.* 70:933
73. Hamel S, Casida ME, Salahub DR. 2002. Exchange-only optimized effective potential for molecules from resolution-of-the-identity techniques: comparison with the local density approximation, with and without asymptotic correction. *J. Chem. Phys.* 116:8276
74. Dreuw A, Weisman JL, Head-Gordon M. 2003. Long-range charge-transfer excited states in time-dependent density functional theory require non-local exchange. *J. Chem. Phys.* 119:2943
75. Peach MJG, Benfield P, Helgaker T, Tozer DJ. 2008. Excitation energies in density functional theory: an evaluation and a diagnostic test. *J. Chem. Phys.* 128:044118
76. Stein T, Kronik L, Baer R. 2009. Reliable prediction of charge transfer excitations in molecular complexes using time-dependent density functional theory. *J. Am. Chem. Soc.* 131:2818
77. Gimon T, Ipatov A, Heßelmann A, Görling A. 2009. Qualitatively correct charge-transfer excitation energies in HeH by time-dependent density-functional theory due to exact exchange Kohn-Sham eigenvalue differences. *J. Chem. Theory Comput.* 5:781
78. Heßelmann A, Ipatov A, Görling A. 2009. Charge-transfer excitation energies with a time-dependent density-functional method suitable for orbital-dependent exchange-correlation functionals. *Phys. Rev. A* 80:012507
79. Mikhailov IA, Tafur S, Masunov AE. 2008. Double excitations and state-to-state transition dipoles in $\pi-\pi^*$ excited singlet states of linear polyenes: time-dependent density-functional theory versus multi-configurational methods. *Phys. Rev. A* 77:012510
80. Casida ME. 2005. Propagator corrections to adiabatic time-dependent density-functional theory linear response theory. *J. Chem. Phys.* 122:054111
81. Gross EKU, Dobson JF, Petersilka M. 1996. Density-functional theory of time-dependent phenomena. *Top. Curr. Chem.* 181:81
82. Tretiak S, Chernyak V. 2003. Resonant nonlinear polarizabilities in the time-dependent density functional theory. *J. Chem. Phys.* 119:8809
83. Isborn CM, Li X. 2007. Modeling the doubly excited state with time-dependent hartree-fock and density functional theories. *J. Chem. Phys.* 129:204107
84. Hirata S, Head-Gordon M, Bartlett RJ. 1999. Configuration interaction singles, time-dependent Hartree-Fock, and time-dependent density functional theory for the electronic excited states of extended systems. *J. Chem. Phys.* 111:10774
85. Champagne B, Perpète EA, van Gisbergen SJA, Baerends EJ, Snijders JG. 1998. Assessment of conventional density functional schemes for computing the polarizabilities and hyperpolarizabilities of conjugated oligomers: an ab initio investigation of polyacetylene chains. *J. Chem. Phys.* 109:10489. Erratum. 1999. *J. Chem. Phys.* 110:1164

86. Champagne B, Perpète EA, Jacquemin D, van Gisbergen SJA, Baerends E, et al. 2000. Assessment of conventional density functional schemes for computing the dipole moment and (hyper)polarizabilities of push-pull π-conjugated system. *J. Phys. Chem. A* 104:4755
87. Petersilka M, Gossmann UJ, Gross EKU. 1996. Excitation energies from time-dependent density-functional theory. *Phys. Rev. Lett.* 76:1212
88. Tawada Y, Tsuneda T, Yanagisawa S, Yanai T, Hirao K. 2004. A long-range-corrected time-dependent density functional theory. *J. Chem. Phys.* 120:8425
89. Tokura S, Tsuneda T, Hirao K. 2006. Long-range-corrected time-dependent density functional study on electronic spectra of five-membered ring compounds and free-base porphyrin. *J. Theor. Comput. Chem.* 5:925
90. Vydrov OA, Scuseria GE. 2006. Assessment of a long-range corrected hybrid functional. *J. Chem. Phys.* 125:234109
91. Peach MJG, Tellgrent EI, Sałek P, Helgaker T, Tozer DJ. 2007. Structural and electronic properties of polvacetylene and polyyne from hybrid and Coulomb-attenuated density functionals. *J. Phys. Chem. A* 111:11930
92. Qian Z, Constantinescu A, Vignale G. 2003. Solving the ultranonlocality problem in time-dependent spin-density-functional theory. *Phys. Rev. Lett.* 90:066402
93. Cave RJ, Zhang F, Maitra NT, Burke K. 2004. A dressed TDDFT treatment of the 2^1A_g states of butadiene and hexatriene. *Chem. Phys. Lett.* 389:39
94. Giesbertz KJH, Baerends EJ. 2008. Failure of time-dependent density functional theory for excited state surfaces in case of homolytic bond dissociation. *Chem. Phys. Lett.* 461:338
95. van Fassen M, de Boeij PL, van Leeuwen R, Berger JA, Snijders JG. 2002. Ultranonlocality in time-dependent current-density-functional theory: application to conjugated polymers. *Phys. Rev. Lett.* 88:186401
96. Varsano D, Marini A, Rubio A. 2008. Optical saturation driven by exciton confinement in molecular chains: a time-dependent density-functional theory approach. *Phys. Rev. Lett.* 101:133002
97. Onida G, Reining L, Rubio A. 2002. Electronic excitations: density-functional versus many-body Green's-function approaches. *Rev. Mod. Phys.* 74:601
98. Reining L, Olevano V, Rubio A, Onida G. 2002. Excitonic effects in solids described by time-dependent density-functional theory. *Phys. Rev. Lett.* 88:066404
99. Sole RD, Adragna G, Olevano V, Reining L. 2003. Long-range behavior and frequency dependence of exchange-correlation kernels in solids. *Phys. Rev. B* 67:045207
100. Kurzweil Y, Baer R. 2004. Time-dependent exchange-correlation current density functionals with memory. *J. Chem. Phys.* 121:8731
101. Wagner LO, Burke K. 2012. Exact conditions and their relevance in TDDFT. See Ref. 7, p. 101
102. Gross EKU, Kohn W. 1985. Local density-functional theory of frequency-dependent linear response. *Phys. Rev. Lett.* 55:2850
103. Vignale G. 2006. Current density-functional theory. See Ref. 167, p. 75
104. Dobson JF, Bünner MJ, Gross EKU. 1997. Time-dependent density functional theory beyond linear response: an exchange-correlation potential with memory. *Phys. Rev. Lett.* 79:1905
105. Kurzweil Y, Baer R. 2008. Adapting approximate-memory potentials for time-dependent density functional theory. *Phys. Rev. B* 77:085121
106. Vignale G, Kohn W. 1996. Current-dependent exchange-correlation potential for dynamical linear response theory. *Phys. Rev. Lett.* 77:2037
107. Vignale G, Ullrich CA, Conti S. 1997. Time-dependent density functional theory beyond the adiabatic local density approximation. *Phys. Rev. Lett.* 79:4878
108. Ullrich CA, Vignale G. 2002. Time-dependent current-density-functional theory for the linear response of weakly disordered systems. *Phys. Rev. B* 65:245102
109. Tokatly IV, Pankratov O. 2003. Local exchange-correlation vector potential with memory in time-dependent density functional theory: the generalized hydrodynamics approach. *Phys. Rev. B* 67:20110
110. Tokatly IV. 2005. Quantum many-body dynamics in a Lagrangian frame: I. Equations of motion and conservation laws. *Phys. Rev. B* 71:165104

111. Tokatly IV. 2005. Quantum many-body dynamics in a Lagrangian frame: II. Geometric formulation of time-dependent density functional theory. *Phys. Rev. B* 71:165105
112. Ullrich CA, Tokatly IV. 2006. Nonadiabatic electron dynamics in time-dependent density-functional theory. *Phys. Rev. B* 73:235102
113. D'Agosta R, Vignale G. 2006. Relaxation in time-dependent current-density-functional theory. *Phys. Rev. Lett.* 96:016405
114. de Boeij PL, Kootstra F, Berger JA, van Leeuwen R, Snijders JG. 2001. Current density functional theory for optical spectra: a polarization functional. *J. Chem. Phys.* 115:1995
115. Nazarov VU, Vignale G, Chang YC. 2010. Communications: on the relation between the scalar and tensor exchange-correlation kernels of the time-dependent density-functional theory. *J. Chem. Phys.* 133:021101
116. Ullrich CA, Grossman UJ, Gross EKU. 1995. Time-dependent optimized effective potential. *Phys. Rev. Lett.* 74:872
117. Görling A. 1998. Exact exchange kernel for time-dependent density-functional theory. *Int. J. Quantum Chem.* 69:265
118. van Leeuwen R. 1996. The Sham-Schlüter equation in time-dependent density-functional theory. *Phys. Rev. Lett.* 76:3610
119. Hirata S, Ivanov S, Grabowski I, Bartlett RJ. 2002. Time-dependent density functional theory employing optimized effective potentials. *J. Chem. Phys.* 116:6468
120. von Barth U, Dahlen NE, van Leeuwen R, Stefanucci G. 2005. Conserving approximations in time-dependent density functional theory. *Phys. Rev. B* 72:235109
121. Bruneval F, Sottile F, Olevano V, Sole RD, Reining L. 2005. Many-body perturbation theory using the density-functional concept: beyond the *GW* approximation. *Phys. Rev. Lett.* 94:186402
122. Huix-Rotllant M, Casida ME. 2010. Formal foundations of dressed time-dependent density-functional theory for many-electron excitations. **http://arxiv.org/abs/1008.1478**
123. Gonze X, Scheffler M. 1999. Exchange and correlation kernels at the resonance frequency: implications for excitation energies in density-functional theory. *Phys. Rev. Lett.* 82:4416
124. Gatti M, Olevano V, Reining L, Tokatly IV. 2007. Transforming nonlocality into a frequency dependence: a shortcut to spectroscopy. *Phys. Rev. Lett.* 057401:1
125. Mearns D, Kohn W. 1987. Frequency-dependent v-representability in density-functional theory. *Phys. Rev. A* 35:4796
126. Hellgren M, von Barth U. 2009. Exact-exchange kernel of time-dependent density functional theory: frequency dependence and photoabsorption spectra of atoms. *J. Chem. Phys.* 131:044110
127. Heßelman A, Görling A. 2011. Efficient exact-exchange time-dependent density-functional theory methods and their relation to time-dependent Hartree-Fock. *J. Chem. Phys.* 134:034120
128. Wijewardane HO, Ullrich CA. 2008. Real-time electron dynamics with exact-exchange time-dependent density-functional theory. *Phys. Rev. Lett.* 100:056404
129. Helbig N, Fuks J, Tokatly I, Appel H, Gross E, Rubio A. 2011. Time-dependent density-functional and reduced density-matrix methods for few electrons: exact versus adiabatic approximations. *Chem. Phys.* 391:1
130. Elliot P, Goldson S, Canahui C, Maitra NT. 2011. Perspectives on double-excitations in TDDFT. *Chem. Phys.* 391:110
131. Romaniello P, Sangalli D, Berger JA, Sottile F, Molinari LG, et al. 2009. Double excitations in finite systems. *J. Chem. Phys.* 130:044108
132. Sangalli D, Romaniello P, Onida G, Marini A. 2011. Double excitations in correlated systems: a many-body approach. *J. Chem. Phys.* 134:034124
133. Maitra NT, Zhang F, Cave FJ, Burke K. 2004. Double excitations within time-dependent density functional theory linear response. *J. Chem. Phys.* 120:5932
134. Huix-Rotllant M, Ipatov A, Rubio A, Casida ME. 2011. Assessment of dressed time-dependent density-functional theory for the low-lying valence states of 28 organic chromophores. *Chem. Phys.* 391:120
135. Pernal K, Giesbertz K, Gritsenko O, Baerends E. 2007. Adiabatic approximation of time-dependent density matrix functional response theory. *J. Chem. Phys.* 127:214101

136. Giesbertz KJH, Baerends EJ, Gritsenko OV. 2008. Charge transfer, double and bond-breaking excitations with time-dependent density matrix functional theory. *Phys. Rev. Lett.* 101:033004
137. Giesbertz KJH, Pernal K, Gritsenko OV, Baerends EJ. 2009. Excitation energies with time-dependent density matrix functional theory: single two-electrons systems. *J. Chem. Phys.* 130:114104
138. Giesbertz K, Gritsenko O, Baerends E. 2010. Response calculations with an independent particle system with an exact one-particle density matrix. *Phys. Rev. Lett.* 105:013002
139. Giesbertz K, Gritsenko O, Baerends E. 2010. The adiabatic approximation in time-dependent density matrix functional theory: response properties from dynamics of phase-including natural orbitals. *J. Chem. Phys.* 133:174119
140. Giesbertz KJH, Baerends EJ. 2010. Aufbau derived from a unified treatment of occupation numbers in Hartree Fock, Kohn Sham, and natural orbital theories with the Karush Kuhn Tucker conditions for the inequality constraints $n_i \leq 1$ and $n_i \geq 0$. *J. Chem. Phys.* 132:194108
141. Casida M. 1999. Reconciling of the ΔSCF and TDDFT approaches to excitation energies in DFT: a charge-transfer correction for TDDFT with GGA functionals. In *Proc. Joint ITP/INT Workshop Time-Dependent Density-Functional Theory.* Santa Barbara, CA: Inst. Theor. Phys., Univ. Calif. St. Barbara. **http://www.itp.ucsb.edu/online/tddft_c99/**
142. Hu C, Sugino O, Miyamoto Y. 2006. Modified linear response for time-dependent density-functional theory: application to Rydberg and charge-transfer excitations. *Phys. Rev. A* 74:032508
143. Hu C, Sugino O. 2007. Average excitation energies from time-dependent density-functional theory. *J. Chem. Phys.* 126:074112
144. Ziegler T, Seth M, Krykunov M, Auschbach J. 2008. A revised electronic Hessian for approximate time-dependent density functional theory. *J. Chem. Phys.* 129:184114
145. Ziegler T, Seth M, Krykunov M, Autschbach J, Wang F. 2009. On the relation between time-dependent and variational density functional theory approaches for the determination of excitation energies and transition moments. *J. Chem. Phys.* 130:154102
146. Ziegler T, Seth M, Krykunov M, Autschbach J, Wang F. 2009. Is charge transfer transition really too difficult for standard density functionals or are they just a problem for time-dependent density functional theory based on a linear response approach? *J. Mol. Struct.* 914:106
147. Ziegler T, Krykunov M. 2010. On the calculation of charge transfer transitions with standard density functionals using constrained variational density functional theory. *J. Chem. Phys.* 133:074104
148. Ziegler T, Krykunov M. 2010. On the calculation of charge transfer transitions with standard density functionals using constrained variational density functional theory. *J. Chem. Phys.* 133:074104
149. Slipchenko LV, Krylov AI. 2003. Electronic structure of the trimethylenemethane diradical in its ground and electronically excited states: bonding, equilibrium geometries, and vibrational frequencies. *J. Chem. Phys.* 118:6874
150. Shao Y, Head-Gordon M, Krylov AI. 2003. The spin-flip approach within time-dependent density functional theory: theory and applications to diradicals. *J. Chem. Phys.* 118:4807
151. Kishi R, Nakano M, Ohta S, Takebe A, Nate M, et al. 2007. Finite-field spin-flip configuration interaction calculation of the second hyperpolarizabilities of singlet diradical systems. *J. Chem. Theory Comput.* 3:1699
152. Thomas A, Srinivas K, Prabhakara C, Bhanuprakasha K, Rao VJ. 2008. Estimation of the first-excitation energy in diradicaloid croconate dyes having absorption in the near-infrared (NIR): a DFT and SF-TDDFT study. *Chem. Phys. Lett.* 454:36
153. Lande ADL, Gérard H, Parisel O. 2008. How to optimize a CH cleavage with a mononuclear copper-dioxygen adduct? *Int. J. Quantum Chem.* 108:1898
154. Minezawa N, Gordon MS. 2009. Optimizing conical intersections by spin-flip density functional theory: application to ethylene. *Phys. Chem. A* 113:12749
155. Wang F, Ziegler T. 2004. Time-dependent density functional theory based on a noncollinear formulation of the exchange-correlation potential. *J. Chem. Phys.* 121:12191
156. Gao J, Zou W, Liu W, Xiao Y, Peng D, et al. 2005. Time-dependent four-component relativistic density functional theory for excitation energies: II. The exchange-correlation kernel. *J. Chem. Phys.* 123:054102
157. Wang F, Ziegler T. 2005. The performance of time-dependent density functional theory based on a noncollinear exchange-correlation potential in the calculation of excitation energies. *J. Chem. Phys.* 122:074109

158. Seth M, Ziegler T. 2005. Calculation of excitation energies of open-shell molecules with spatially degenerate ground states. I. Transformed reference via an intermediate configuration Kohn-Sham density-functional theory and applications to d^1 and d^2 systems with octahedral and tetrahedral symmetries. *J. Chem. Phys.* 123:144105
159. Guan J, Wang F, Ziegler T, Cox H. 2006. Time-dependent density functional study of the electronic potential energy curves and excitation spectrum of the oxygen molecule. 125:044314
160. Seth M, Mazur G, Ziegler T. 2011. Time-dependent density functional theory gradients in the Amsterdam density functional package: geometry optimizations of spin-flip excitations. *Theor. Chem. Acc.* 129:331
161. Vahtras O, Rinkevicius Z. 2007. General excitations in time-dependent density functional theory. *J. Chem. Phys.* 126:114101
162. Rinkevicius Z, Ågren H. 2010. Spin-flip time dependent density functional theory for singlet-triplet splittings in σ,σ-biradicals. *Chem. Phys. Lett.* 491:132
163. Li Z, Liu W. 2010. Spin-adapted open-shell random phase approximation and time-dependent density functional theory. I. Theory. 133:064106
164. Li Z, Liu W, Zhang Y, Suo B. 2011. Spin-adapted open-shell time-dependent density functional theory. II. Theory and pilot application. *J. Chem. Phys.* 134:134101
165. Ipatov A, Cordova F, Doriol LJ, Casida ME. 2009. Excited-state spin-contamination in time-dependent density-functional theory for molecules with open-shell ground states. *J. Mol. Struct.* 914:60
166. Rinkevicius Z, Vahtras O, Ågren H. 2010. Spin-flip time-dependent density-functional theory applied to excited states with single-, double-, or mixed-electron excitation character. *J. Chem. Phys.* 133:114104
167. Marques MAL, Ullrich C, Noguieria F, Rubio A, Gross EKU, eds. 2006. *Time-Dependent Density-Functional Theory.* Lect. Notes Phys. Vol. 706. Berlin: Springer

Annual Review of
Physical Chemistry
Volume 63, 2012

Contents

Indexes

Errata

An online log of corrections to Annual Review of Physical Chemistry chapters (if any, 1997 to the present) may be found at http://physchem.AnnualReviews.org/errata.shtml